Received: 9 November 2017 | Revised: 23 March 2018 | Accepted: 26 March 2018

DOI: 10.1111/mec.14699

INVITED REVIEWS AND SYNTHESES

WILEY MOLECULAR ECOLOGY

# Meta-analysis of chromosome-scale crossover rate variation in eukaryotes and its significance to evolutionary genomics

Quiterie Haenel[1]* | Telma G. Laurentino[1]* | Marius Roesti[2] | Daniel Berner[1]

[1]Zoological Institute, University of Basel, Basel, Switzerland

[2]Department of Zoology, University of British Columbia, Vancouver, BC, Canada

**Correspondence**
Daniel Berner, Zoological Institute, University of Basel, Basel, Switzerland.
Email: daniel.berner@unibas.ch

**Funding information**
Janggen-Pöhn Foundation; Schweizerischer Nationalfonds zur Förderung der Wissenschaftlichen Forschung, Grant/Award Number: 31003A_165826

## Abstract

Understanding the distribution of crossovers along chromosomes is crucial to evolutionary genomics because the crossover rate determines how strongly a genome region is influenced by natural selection on linked sites. Nevertheless, generalities in the chromosome-scale distribution of crossovers have not been investigated formally. We fill this gap by synthesizing joint information on genetic and physical maps across 62 animal, plant and fungal species. Our quantitative analysis reveals a strong and taxonomically widespread reduction of the crossover rate in the centre of chromosomes relative to their peripheries. We demonstrate that this pattern is poorly explained by the position of the centromere, but find that the magnitude of the relative reduction in the crossover rate in chromosome centres increases with chromosome length. That is, long chromosomes often display a dramatically low crossover rate in their centre, whereas short chromosomes exhibit a relatively homogeneous crossover rate. This observation is compatible with a model in which crossover is initiated from the chromosome tips, an idea with preliminary support from mechanistic investigations of meiotic recombination. Consequently, we show that organisms achieve a higher genome-wide crossover rate by evolving smaller chromosomes. Summarizing theory and providing empirical examples, we finally highlight that taxonomically widespread and systematic heterogeneity in crossover rate along chromosomes generates predictable broad-scale trends in genetic diversity and population differentiation by modifying the impact of natural selection among regions within a genome. We conclude by emphasizing that chromosome-scale heterogeneity in crossover rate should urgently be incorporated into analytical tools in evolutionary genomics, and in the interpretation of resulting patterns.

**KEYWORDS**
centromere, chromosome length, gene density, linked selection, meiosis, recombination

## 1 | INTRODUCTION

Meiosis is a specialized cell division widely conserved among sexually reproducing eukaryotes, involving one round of DNA replication followed by two rounds of chromosome division, thus producing haploid cells (gametes, spores) from diploid progenitors. During the first meiotic division, homologous chromosomes pair and undergo recombination. This involves numerous programmed DNA double-strand breaks and the invasion of short single-stranded DNA segments into the homologous chromosome. A small fraction of the DNA breaks are then repaired as crossovers (CO), the reciprocal exchange of DNA segments between the homologous chromosomes (Hunter, 2007; CO is thus only one aspect of recombination, and hence, these two terms are not used interchangeably in this study). CO is an intriguing biological process because of its dual mechanistic and evolutionary implications. On the one hand, the segregation of

*Quiterie Haenel and Telma G. Laurentino share first authorship, alphabetical order.

  

chromosomes during the first meiotic division requires that homologous chromosomes associate physically to align together on the meiotic spindle in the cell's equator, which is facilitated by CO (or chiasma, the cytological manifestation of CO). CO is thus important for proper chromosome disjunction. Although exceptions exist (e.g., the absence of CO in some dipteran males or lepidopteran females; Gerton & Hawley, 2005; Wolf, 1994), one obligate CO per chromosome pair is generally considered a requirement for accurate chromosome segregation and hence the production of genetically balanced offspring (Hassold & Hunt, 2001; Hunter, 2007; Mather, 1938; Smith & Nicolas, 1998).

On the other hand, CO also has crucial evolutionary consequences: by breaking and interchanging DNA segments from two homologous chromosomes, CO generates novel combinations of alleles. A possible benefit of this genetic reshuffling is that favourable alleles initially occurring on different copies of a given chromosome can be unified into a single chromosome. This chromosome combines the selective benefit of all the alleles it carries, and hence represents a genotype of higher fitness than what would be possible in the absence of CO. CO thus increases genetic variance among individuals, therefore making natural selection in finite populations more efficient (Burt, 2000; Felsenstein, 1974; Fisher, 1930; Hartfield & Otto, 2011; Hill & Robertson, 1966; Kondrashov, 1982; Muller, 1932; Otto & Barton, 1997, 2001)—an effect providing a general explanation for the evolutionary benefit of sexual over asexual reproduction. However, the increase in genetic variation due to CO can also entail a reduction in the mean fitness of a population, for instance when favourable epistatic interactions among loci are broken down (Barton, 1995; Fisher, 1930), or when populations adapted to selectively different habitats hybridize and locally favourable and unfavourable alleles become associated (Barton & Bengtsson, 1986; Berner & Roesti, 2017; Kirkpatrick & Barton, 2006; Ortiz-Barrientos, Reiland, Hey, & Noor, 2002).

The evolutionary consequences of CO depend strongly on the distribution of CO along chromosomes. At a fine scale, the CO rate is often dramatically elevated in localized "hotspots" (Baudat, Imai, & de Massy, 2013; Choi & Henderson, 2015; Lichten & Goldman, 1995). While the distribution of hotspots and their molecular control are under intensive investigation, less attention has been paid to the distribution of CO along chromosomes at a broad scale. In several organisms, it has long been noticed that the CO rate differs greatly among broad chromosome regions (Akhunov et al., 2003; Croft & Jones, 1989; International Human Genome Sequencing Consortium 2001; Nachman & Churchill, 1996; Rahn & Solari, 1986; Rees & Dale, 1974), but so far, no attempt has been made to formally examine the distribution of CO at a large chromosomal scale across taxa.

The objective of this study is to fill this gap by exploiting the recent proliferation of well-characterized CO landscapes in higher eukaryotes (animals, plants, fungi) driven by progress in genome sequencing and marker generation techniques. Using a meta-analytical approach, we document a widespread trend of CO to occur at a relatively elevated rate in the chromosome peripheries. We address the mechanisms potentially causing this pattern and highlight why appreciating this nonrandom distribution of CO across the genome is important to evolutionary population genomics.

## 2 | METHODS

### 2.1 | Data acquisition

To initiate our meta-analysis, we conducted a literature search for studies characterizing the distribution of CO across the genome. We considered two types of data sets: first, studies reporting the genetic map position of genetic markers along with their physical base pair position along chromosomes, that is, centimorgan (cM) vs. megabase (Mb) data (>80% of the data sets eventually used). Second, we also considered studies directly reporting CO rates along chromosomes quantified as genetic map distance divided by physical map distance for marker intervals (i.e., cM/Mb vs. Mb data). Our focus was on organisms with an assembled genome (in a few cases, this genome was from a close congeneric species) and with CO rates estimated from crosses or pedigrees. Studies estimating CO rates from linkage disequilibrium in population samples, presenting information from a single chromosome only, or performed with low marker resolution (fewer than ~20 markers per chromosome on average) were ignored. In a single case (Nunes et al., 2017), we considered a marker-dense data set presenting genetic map position against marker order (instead of Mb position in a physical assembly). Visually comparing patterns of cM vs. Mb to cM vs. marker order in another organism in which both data types were available (Dohm et al., 2012, 2014) confirmed that the latter data type also reliably captures broad-scale CO patterns (see also Nachman & Churchill, 1996). All species were assigned to the categories "wild" or "domesticated", the latter subsuming all systems at least potentially having experienced selection by humans (i.e., domesticated, cultivated or classical laboratory model organisms). For species in which suitable CO data were available from multiple independent investigations, we prioritized the study with the most reliable genome assembly and/or the highest marker resolution.

In some studies, the relevant raw data were presented directly in tabulated form. Otherwise, we extracted information from graphics using *webplotdigitizer* (http://arohatgi.info/WebPlotDigitizer). In graphics permitting the identification of individual raw data points, the latter were digitized directly. When marker resolution was relatively sparse, we considered all available data points (ignoring obvious outliers caused by genome misassembly). In high-resolution studies with heavily overlapping data points, we digitized only a subset of points per chromosome sufficient to capture broad-scale CO patterns accurately (a few such data sets digitized independently by multiple researchers confirmed that this subsampling produced highly reproducible CO rate data). In cases where the data were presented as line graphics (e.g., smoothed profiles along chromosomes), and hence, the raw data were not accessible, we superposed a grid of equidistant lines orthogonal to the Mb axis on the plot of each chromosome and digitized the intersections between grid and data lines. This grid was adjusted to span the entire chromosome and included either 26 lines for cM vs. Mb plots, or 25 lines for cM/Mb vs. Mb

plots, eventually yielding CO rate estimates for a minimum of 25 windows along each chromosome across all studies. In studies providing CO information separately for both sexes or for multiple crosses, data were extracted separately for each category and then averaged for analysis (note that in *Drosophila*, CO occurs only in females; we nevertheless considered this species for analysis, although excluding it did not influence any conclusion). To avoid bias by unusual patterns of CO in sex chromosomes, we restricted data acquisition to autosomes in those studies identifying a sex chromosome. In a few studies, a subset of chromosomes had to be ignored because they showed massive macro-assembly problems (large marker gaps, or genetic map position failing to increase monotonically over large chromosome regions). All raw data sets are available on the Dryad repository (https://doi.org/10.5061/dryad.p1j7n43).

## 2.2 | Characterizing the broad-scale distribution of CO across taxa

A first goal was to visualize the broad-scale distribution of CO along chromosomes across all species within each of the three organismal kingdoms (animals, plants, fungi). For studies providing cM vs. Mb data, this initially required calculating the CO rate (cM/Mb) for intervals of adjacent markers. To achieve comparability, physical midpoint positions of marker intervals were then scaled according to a standard chromosome length of one, and CO rates were divided by their respective chromosome average rate (i.e., mean-standardized, Houle, 1992; qualitatively similar results leading to the same conclusions were obtained by standardizing CO rates by the chromosome-specific standard deviation, or by performing no standardization at all). These adjustments made variation in CO rate within chromosomes independent from differences in physical length and in absolute CO rate among chromosomes and organisms. Within each species, we next combined standardized CO rates from all chromosomes according to their relative chromosome position. For this, we assigned CO rate data points from all chromosomes (scaled to unit length) to one of 25 adjacent windows and computed for each window the median CO rate across chromosomes (using the mean to combine the data points within an organism produced similar result). Finally, the species-specific CO rates thus summarized were averaged across species within each kingdom for each of the 25 chromosome windows for visualization (data available as Appendix S2). We also calculated 95% confidence intervals (CIs) around the window-specific means by bootstrap resampling among the species 10,000 times (Manly, 2007; throughout the study, CIs around point estimates were calculated analogously). For selected species, we also visualized the standardized CO rate along an exemplary chromosome at the original marker resolution and physical chromosome scale.

## 2.3 | Influence of the centromere on the broad-scale distribution of CO

The above analysis revealed a general broad-scale reduction in CO rate across the centres of chromosomes (see Section 3). To gain insights into potential underlying causes, we explored to what extent this heterogeneity in CO rate is related to the position of the centromere, a chromosome region essential for proper chromosome segregation and exhibiting a reduced CO rate (Talbert & Henikoff, 2010). This analysis focused on the subset of species for which centromere positions were available. These positions had to be inferred from DNA sequence motifs or other physical markers, not from the distribution of CO. We further ignored species with short chromosomes (less than ~20 Mb on average), because we found that pronounced broad-scale heterogeneity in CO rate was often lacking on short chromosomes (see Section 3), thus precluding a meaningful analysis of the centromere's role in driving such heterogeneity. In the 17 total species satisfying these criteria (Table 1; references to the studies characterizing centromere position in these species are given in Table S1), we assigned all chromosomes to one of six total morphological categories. These included metacentric, submetacentric, subtelocentric, acrocentric and telocentric chromosomes, as defined by a decreasing ratio of the short to the long chromosome arm (Levan, Fredga, & Sandberg, 1964). These five categories thus provide a crude description of how central or peripheral the centromere is located within a chromosome. The sixth category was the holocentric chromosomes lacking a single well-defined centromere. Here the spindle fibres guiding chromosome segregation can attach along the entire chromosome (Dernburg, 2001; Melters, Paliulis, Korf, & Chan, 2012). To assess whether the broad-scale reduction in CO rate across chromosome centres is determined by centromere position, we took two qualitative, visual approaches (quantitative analysis was precluded by heterogeneity in the quality of centromere position information across studies): first, we focused on species with the same morphology across all chromosomes. For these species, we graphed the median standardized CO rate for each of the 25 chromosome windows as described above and then compared the distribution of the CO rate between species differing in chromosome morphology. The second approach focused on different chromosome morphologies occurring *within* species. We here again plotted window-specific standardized CO rates, but this time separately for each chromosome morphology category within a species (at least three chromosomes per morphological category were required). In both analyses, our prediction was that if the centromere position determines the broad-scale CO landscape, chromosomes exhibiting peripheral centromeres should lack a systematic reduction in CO rate around chromosome centres.

## 2.4 | Relationship between CO rate and chromosome length

Observations during data acquisition raised the possibility that the strength of the reduction in CO rate within chromosome centres relative to peripheries (see Section 3) could be related to chromosome length. This idea was investigated both among and within species. For the former, we reused the standardized CO rates calculated for each chromosome in each species as described above. For each chromosome, we calculated the mean CO rate across all

**TABLE 1** Species of higher eukaryotes included in our meta-analysis of crossover rate, sorted by organismal kingdom and class (animals) or family (plants)

| Kingdom | Class/Family | Species | Common name | Author |
|---|---|---|---|---|
| Animals | Actinopterygii | *Colossoma macropomum* | Tambaqui | Nunes et al. (2017) |
| Animals | Actinopterygii | *Cyprinus carpio* | Carp | Xu et al. (2014) |
| Animals | Actinopterygii | *Danio rerio* | Zebrafish | Bradley et al. (2011) |
| Animals | Actinopterygii | *Gasterosteus aculeatus*[w,c] | Threespine stickleback | Roesti et al. (2013) |
| Animals | Actinopterygii | *Ictalurus punctatus* | Catfish | Liu et al. (2016) |
| Animals | Actinopterygii | *Lates calcarifer*[w] | Asian seabass | Wang et al. (2017) |
| Animals | Aves | *Ficedula albicollis*[w] | Collared flycatcher | Kawakami et al. (2014) |
| Animals | Aves | *Gallus gallus* | Chicken | Groenen et al. (2009) |
| Animals | Aves | *Taeniopygia guttata* | Zebra finch | Backström et al. (2010) |
| Animals | Branchiopoda | *Daphnia magna*[w] | Daphnia | Dukić, Berner, Roesti, Haag, and Ebert (2016) |
| Animals | Chromadorea | *Caenorhabditis briggsae*[c] | Nematode | Ross et al. (2011) |
| Animals | Chromadorea | *Caenorhabditis elegans*[c] | Nematode | Rockman and Kruglyak (2009) |
| Animals | Insecta | *Aedes aegypti*[w,c] | Yellow fever mosquito | Juneja et al. (2014) |
| Animals | Insecta | *Apis mellifera* | Honeybee | Solignac et al. (2007) |
| Animals | Insecta | *Bactrocera cucurbitae* | Melon fly | Sim and Geib (2017) |
| Animals | Insecta | *Bombus terrestris*[w] | Bumblebee | Liu et al. (2017) |
| Animals | Insecta | *Drosophila melanogaster* | Fruit fly | Comeron, Ratnappan, and Bailin (2012) |
| Animals | Insecta | *Heliconius melpomene*[w,c] | Postman butterfly | Davey et al. (2016) |
| Animals | Insecta | *Laupala kohalensis x paranigra*[w] | Cricket | Blankers, Oh, Bombarely, and Shaw (2017) |
| Animals | Insecta | *Nasonia vitripennis*[w,c] | Wasp | Niehuis et al. (2010) |
| Animals | Mammalia | *Bos taurus*[c] | Cattle | Arias, Keehan, Fisher, Coppieters, and Spelman (2009) |
| Animals | Mammalia | *Canis lupus familiaris*[c] | Dog | Wong et al. (2010) |
| Animals | Mammalia | *Cervus elaphus*[w,c] | Red deer | Johnston et al. (2017) |
| Animals | Mammalia | *Felis catus*[c] | Cat | Li et al. (2016) |
| Animals | Mammalia | *Homo sapiens*[w,c] | Human | Jensen-Seaman et al. (2004) |
| Animals | Mammalia | *Mus musculus*[c] | Mouse | Jensen-Seaman et al. (2004) |
| Animals | Mammalia | *Ovis aries*[c] | Sheep | Johnston et al. (2016) |
| Animals | Mammalia | *Pan troglodytes verus*[w,c] | Chimpanzee | Auton et al. (2012) |
| Animals | Mammalia | *Rattus norvegicus*[c] | Rat | Jensen-Seaman et al. (2004) |
| Animals | Mammalia | *Sus scrofa* | Pig | Tortereau et al. (2012) |
| Fungi | Dothideomycetes | *Zymoseptoria tritici*[w] | | Croll, Lendenmann, Stewart, and McDonald (2015) |
| Fungi | Saccharomycetes | *Saccharomycetes cerevisiae* | Baker's yeast | Cherry et al. (2012) |
| Fungi | Sordariomycetes | *Fusarium graminearum*[w] | | Laurent et al. (2017) |
| Plants | Amaranthaceae | *Beta vulgaris*[c] | Sugar beet | Dohm et al. (2014) |
| Plants | Asteraceae | *Helianthus annuus* | Sunflower | Renaut et al. (2013) |
| Plants | Brassicaceae | *Arabidopsis thaliana* | Thale cress | Giraut et al. (2011) |
| Plants | Brassicaceae | *Brassica napus* | Rapeseed | Wang et al. (2015b) |
| Plants | Brassicaceae | *Brassica rapa* | Chinese cabbage | Huang, Yang, Zhang, and Cao (2017) |
| Plants | Cucurbitaceae | *Citrullus lanatus* | Watermelon | Ren et al. (2012) |
| Plants | Cucurbitaceae | *Cucumis melo* | Melon | Argyris et al. (2015) |
| Plants | Fabaceae | *Cicer arietinum* | Chickpea | Deokar et al. (2014) |
| Plants | Fabaceae | *Glycine max* | Soybean | Schmutz et al. (2010) |
| Plants | Fabaceae | *Phaseolus vulgaris*[c] | Common bean | Bhakta, Jones, and Vallejos (2015) |
| Plants | Juglandaceae | *Juglans regia*[w] | Walnut | Luo et al. (2015) |
| Plants | Malvaceae | *Gossypium hirsutum* | Cotton | Wang et al. (2015a) |

(Continues)

**TABLE 1** (Continued)

| Kingdom | Class/Family | Species | Common name | Author |
|---|---|---|---|---|
| Plants | Malvaceae | *Theobroma cacao* | Cocoa | Argout et al. (2011) |
| Plants | Phrymaceae | *Mimulus guttatus*[w] | Monkey flower | Holeski et al. (2014) |
| Plants | Poaceae | *Brachypodium distachyon* | Purple false brome | Huo et al. (2011) |
| Plants | Poaceae | *Oryza sativa* | Rice | Tian et al. (2009) |
| Plants | Poaceae | *Setaria italica* | Foxtail millet | Zhang et al. (2012) |
| Plants | Poaceae | *Sorghum bicolor* | Sorghum | Bekele, Wieckhorst, Friedt, and Snowdon (2013) |
| Plants | Poaceae | *Triticum aestivum* | Wheat | Gardner, Wittern, and Mackay (2016) |
| Plants | Poaceae | *Zea mays* | Maize | Bauer et al. (2013) |
| Plants | Rosaceae | *Fragaria vesca* | Woodland strawberry | Shulaev et al. (2011) |
| Plants | Rosaceae | *Malus pumila* | Apple | Daccord et al. (2017) |
| Plants | Rosaceae | *Prunus persica* | Peach | International Peach Genome Initiative (2013) |
| Plants | Rutaceae | *Citrus clementina* | Clementine | Wu et al. (2014) |
| Plants | Salicaceae | *Populus deltoides* | Eastern cottonwood | Tong et al. (2016) |
| Plants | Salicaceae | *Populus simonii* | Simon poplar | Tong et al. (2016) |
| Plants | Solanaceae | *Capsicum annuum* | Pepper | Hill et al. (2015) |
| Plants | Solanaceae | *Solanum lycopersicum* | Tomato | Tomato Genome Consortium (2012) |
| Plants | Solanaceae | *Solanum tuberosum* | Potato | Endelman and Jansky (2016) |

Superscripts following species names indicate studies in which the crosses or pedigrees underlying genetic mapping were derived from wild individuals (*w*), and for which information on centromere position was available (*c*).

marker intervals having their physical mid-point within 10 Mb from either chromosome tip (using 5 Mb only produced very similar results) and divided this value by the chromosome-wide average CO rate. The resulting "CO periphery-bias" provided a standardized descriptor of the CO distribution along a chromosome, with a value near one indicating a relatively evenly distributed CO rate, and greater positive values indicating a concentration of CO towards the chromosome tips. Next, we defined the length of each chromosome as the Mb position of the terminal marker interval mid-point, calculated mean CO periphery-bias and chromosome length across the chromosomes within each species and assessed if chromosome length predicted the CO distribution when using species as data points. This was carried out using Spearman's rank correlation (hereafter simply "correlation" because we always applied the Spearman method to quantify the strength of association between variables) and included all species except the single one lacking physical chromosome positions (Nunes et al., 2017). The correlation between CO periphery-bias and chromosome length was further explored *within* species (i.e., using chromosomes as data points). To ensure sufficient sensitivity, this latter analysis was restricted to species represented by at least six chromosomes in our data set, exhibiting at least one chromosome longer than 30 Mb, and showing an at least twofold length difference between the shortest and longest chromosome. The distribution of species-specific correlation coefficients was then evaluated within animals ($N = 16$) and plants ($N = 11$) separately (the species used for this analysis are listed in Appendix S3). To confirm the adequacy of our CO periphery-bias metric, we repeated the above analyses by quantifying the distribution of CO along a chromosome using two alternative methods: the coefficient of a quadratic regression of standardized CO rate vs. Mb position and the ratio of mean peripheral to central CO rate based on the crude centre-periphery delimitation used in Berner and Roesti (2017). All these analyses produced qualitatively similar results supporting the same conclusions, so we report only results obtained with the main method (data available as Appendix S3).

Because the above analysis indicated that the CO distribution within chromosomes was related to chromosome length, we next explored whether chromosome length also predicted the average chromosome-wide CO rate (i.e., cM/Mb across the entire chromosome, ignoring *within*-chromosome heterogeneity). Again, this analysis was performed among and within species (data available as Appendix S4). For the former, we cumulated genetic and physical map length across all chromosomes of each species in our data set for which raw cM information was available ($N = 52$). Dividing total cumulative genetic map length by its physical counterpart then yielded an estimate of the average CO rate for a chromosome—and of the average CO rate across the entire genome—in a given species. Finally, we examined if this quantity was related to median chromosome length when using species as data points. In an analogous analysis within species, we divided genetic by physical map length for each chromosome and calculated the correlation between this average CO rate and physical length across chromosomes within each species represented by at least six chromosomes in our data set. The distribution of correlation coefficients was then evaluated across species separately within each kingdom.

## 2.5 | Relationship between CO rate and gene density

A major evolutionary consequence of CO is that selectively relevant genetic variation from multiple copies of a given chromosome can be recombined. The efficacy of this process depends on the distribution of CO relative to the distribution of genetic information units along chromosomes. Our finding of heterogeneity in the distribution of CO thus raised the important question whether the density of genes is also heterogeneous at the scale of entire chromosomes. To explore this question, we first retrieved data from BIOMART (http://www.biomart.org) on the physical location of protein-coding genes along chromosomes (considering only autosomes, when known) in all species with annotated genomes (16 animals, 14 plants, 3 fungi; total $N = 33$). The broad-scale distribution of gene density was then characterized analogously to the distribution of CO along chromosomes: each chromosome in each species was scaled to unit length and divided into 25 windows of equal width, and the number of genes falling into each window was determined. Variation in gene density among species, and among chromosomes within species, was accounted for by scaling window-specific gene counts along a given chromosome by the mean number of genes across all windows on that chromosome. Relative gene density thus obtained was then summarized for each species by calculating the median value over all chromosomes for each of the 25 windows. Finally, we averaged the species-specific relative gene densities for each window and estimated the associated 95% bootstrap CIs, separately for each kingdom. In addition, we quantified the strength of the association between gene density and CO rate within each animal and plant species by the correlation coefficient calculated with window-specific median values as data points, and evaluated the distribution of this statistic in both kingdoms (due to small sample size, this distribution was again not evaluated in fungi). We note that these analyses made the assumption that the density of potential selective targets in a chromosome region can be expressed based on gene counts. This assumption appears reasonable, given a strong correspondence between gene number and total coding sequence length at least at a broad scale (Berner & Roesti, 2017).

## 2.6 | Relationship between CO rate and the magnitude of population differentiation

In a final set of analyses, we examined how the interaction between broad-scale heterogeneity in CO rate and divergent natural selection can influence patterns of genetic differentiation in genome-wide marker-based population comparisons. We here reused single nucleotide polymorphism (SNP) data generated through RAD sequencing in threespine stickleback fish (*Gasterosteus aculeatus*) adapted to ecologically different habitats (ocean, lake, stream) in the Vancouver Island region (Canada; Roesti, Gavrilets, Hendry, Salzburger, & Berner, 2014; Roesti, Hendry, Salzburger, & Berner, 2012). Specifically, we focused on a pair of populations that diverged between the lake and its adjacent outlet stream habitat in the Boot Lake watershed (our "lake–stream" population comparison), and a pair involving a marine and a geographically close freshwater (stream-resident) population (Sayward estuary and Robert's stream; our "marine–freshwater" population comparison). Detailed information on the ecology and adaptive divergence of these populations and on the generation of the SNP data is provided in Berner, Adams, Grandchamp, and Hendry (2008), Berner, Grandchamp, and Hendry (2009) and Roesti et al. (2012, 2014). For both population comparisons, SNPs were first quality filtered as described in Roesti et al. (2014) and then used to calculate the absolute allele frequency difference (AFD) as a simple metric of population differentiation (Shriver et al., 1997). Considering data from the 20 autosomes only (i.e., the known sex chromosome was excluded) and using only the one SNP per RADtag producing the highest AFD, we obtained differentiation values from 3,622 SNPs for the lake–stream and 9,351 SNPs for the marine–freshwater comparison. Given a genome size of ~460 Mb for threespine stickleback (Jones et al., 2012), the marker resolution in these data sets was relatively low (the expected spacing between SNPs was ~130 and 50 kb) but still sufficient to characterize broad-scale trends in population differentiation (Roesti et al., 2012, 2014).

We first generated differentiation profiles along chromosomes for each population comparison, averaging AFD values from individual SNPs across nonoverlapping sliding windows of 1 Mb. Next, we assessed to what extent differentiation values were correlated between the two—ecologically different (lake–stream vs. marine–freshwater)—population comparisons. For this, we calculated the correlation between the two comparisons across all nonoverlapping, genome-wide sliding windows, considering different window sizes: 0.1, 0.2, 0.5, 1, 2, 3 and 4 Mb. As this analysis revealed an increasingly strong correlation between the two differentiation profiles with increasing window size (see Section 3), we hypothesized that increasing window size should also lead to a stronger genome-wide association between CO rate and differentiation within each population comparison. We tested this prediction by calculating the average CO rate for all windows based on genome-wide CO rate data from Roesti, Moser, and Berner (2013) and quantified how strongly this variable was correlated with the average population differentiation calculated for the same windows. As above, this procedure was repeated for different window sizes ranging from 0.1 to 4 Mb. Finally, our observation that heterogeneity in the distribution of CO is related to their physical length (see Section 3) motivated two analyses focusing on the relationship between chromosome length and the magnitude of population differentiation. In the first analysis, we calculated for each of the two population comparisons the chromosome-specific overall magnitude of genetic differentiation based on the median AFD value across all SNPs on a chromosome. Then, we calculated the correlation between overall differentiation and chromosome length separately for each population comparison. In the second analysis, we defined the SNPs from the top 5% of the genome-wide AFD distribution in each population comparison as "high-differentiation SNPs" and calculated for each chromosome the proportion of high-differentiation SNPs among the total SNPs on that chromosome (thus accounting for different absolute SNP numbers among chromosomes). Then, we tested if this proportion

was correlated to chromosome length. All these analyses excluded the sex chromosome (19), and additionally chromosome 21; the latter because this chromosome harbours a large (>2 Mb) inversion (Jones et al., 2012; Roesti, Kueng, Moser, & Berner, 2015) confounding the broad-scale CO distribution (including chromosome 21 did not qualitatively change any conclusion). All analyses and plotting were performed with R (R Core Team 2017); codes are available upon request.

## 3 | RESULTS AND DISCUSSION

### 3.1 | Data set for meta-analysis

Our literature search identified 62 species in which CO rates were linked to chromosome-level genome assemblies, including 30 animals, 29 plants and 3 fungi (Table 1). Our data set is thus well suited for generalizations about the CO landscape in animals and plants, but less so in the fungal kingdom. The data set is clearly dominated by species of economic relevance and laboratory model systems, which is not surprising, given that generating a chromosome-level genome assembly remains a substantial investment. For the vast majority of species (>90%), CO information suitable to this study was available in graphical form only. To facilitate future investigations, we encourage authors to publish raw genetic map positions in cM together with physical Mb positions for all markers in tabulated and hence more easily accessible form.

### 3.2 | Reduced CO rate in chromosome centres is a major trend in eukaryotes

Our meta-analysis revealed a striking broad-scale pattern across the animal and plant data sets: chromosome centres displayed a dramatically reduced CO rate compared to the chromosome peripheries (Figure 1). In animals, the rate of peripheral CO was more than 2.5 times higher than the CO rate in the central region of chromosomes, and in plants, this difference was more than fivefold. Animals further displayed a clear drop in CO rate towards the very tips of the chromosomes. Additional exploration of the plant data (including filtering for those species with the highest marker resolution and with annotated and hence probably high-quality genomes, and considering different chromosome length classes; details not presented) strongly suggested that the absence of a (strong) terminal drop in CO rate in plants is real, and not an artefact. In contrast to animals and plants, fungal species did not exhibit a clear broad-scale trend in the distribution of CO, although the data for this organismal kingdom were sparse. To ensure that the pattern seen in animals and plants was not driven by specific taxonomic groups, we additionally analysed data separately for all animal classes and plant families listed in Table 1, provided they were represented by at least three different genera (i.e., ray-finned fishes [Actinopterygii], birds, insects and mammals; Fabaceae, Poaceae and Rosaceae). This confirmed that a reduced CO rate in chromosome centres is taxonomically widespread within the animal and plant kingdoms (Figure S1 in Appendix S1). In addition, we examined if there was an influence of artificial selection on the distribution of CO. The motivation was that strong selection and small population size—typical conditions under domestication—are expected theoretically to impose indirect selection on genetic variants that increase the CO rate (Barton & Otto, 2005), a prediction with mixed empirical support (Burt & Bell, 1987; Muñoz-Fuentes et al., 2015; Rees & Dale, 1974; Ross-Ibarra, 2004). While we see no reason why domestication should drive consistent evolution in the *physical location* of CO along chromosomes, we nevertheless graphed the average CO landscape for the pool of all

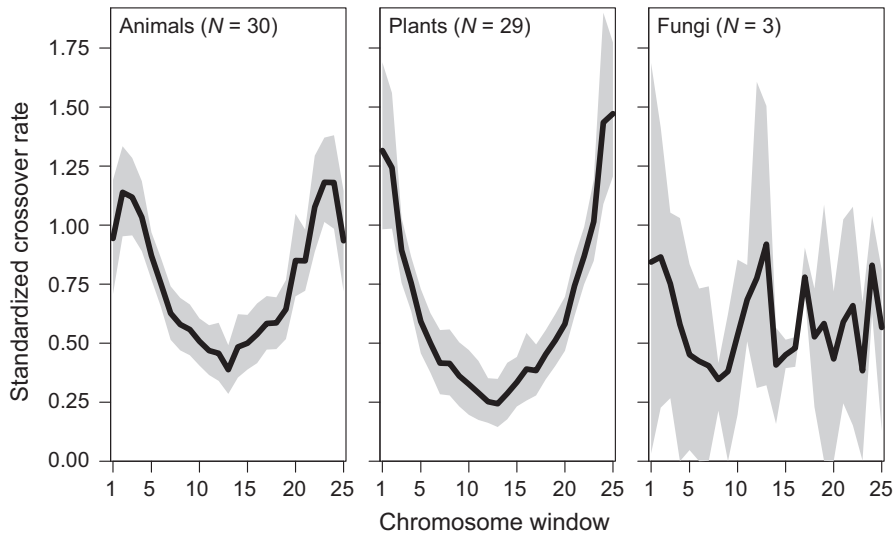


**FIGURE 1** Broad-scale heterogeneity in crossover (CO) rate along chromosomes in eukaryotes. Black lines show the average CO rate across all species within each organismal kingdom (sample sizes in parentheses) along chromosomes divided into 25 windows. Associated 95% bootstrap confidence bands are shaded in grey (in fungi with low sample size, this band reflects the data range). To achieve comparability among study systems, all chromosomes were first scaled to unit length and CO rates were mean standardized across windows within each chromosome, and then, the median value per window was calculated across all chromosomes within each species

animals classified as wild ($N = 12$, Table 1; a meaningful analogous analysis in plants was precluded by the low number of wild species, $N = 2$). Wild animals also exhibited the strong reduction in CO rate in chromosome centres observed across the complete data sets (Figure S1), ruling out domestication as an explanation for the observed trend in the distribution of CO.

### 3.3 | Broad-scale heterogeneity in CO rate is not well explained by centromere position

An intuitive explanation for CO to occur primarily towards the peripheries of a chromosome is that CO may be inhibited in the chromosome's centres if this region harbours the centromere. The centromere is a chromosome region typically characterized by a core of DNA sequence repeats serving as the assembly site of the kinetochore, a protein complex to which the spindle fibres required for proper chromosome segregation attach. In addition, the centromere is possibly also involved in chromosome sorting during the very early stages of meiosis (Allshire & Karpen, 2008; Da Ines, Gallego, & White, 2014; Malik & Henikoff, 2009; McFarlane & Humphrey, 2010; Zickler & Kleckner, 2016). Around the centromere, CO is well known to be suppressed (Beadle, 1932; Harushima et al., 1998; Lambie & Roeder, 1986; Mahtani & Willard, 1998; Rahn & Solari, 1986; Sherman & Stack, 1995). In yeast, for instance, molecular components of the kinetochore complex inhibit DNA double-strand breaks—a necessary precursor of CO—near the centromere and prevent DNA breaks in the broader neighbourhood of the centromere to be repaired as CO (Ellermeier et al., 2010; Vincenten et al., 2015).

Two aspects of centromeres, however, challenge their general importance as determinants of the broad-scale chromosomal distribution of CO across species. The first is the centromeres' relatively small size. Consequently, centromere-associated CO suppression may be a relatively localized phenomenon within a chromosome only. Indeed, CO inhibition extends over just a few kilobases around the centromere in budding yeast (Vincenten et al., 2015), and over 2.3 Mb on a rice chromosome investigated (Yan et al., 2005). It is thus not evident how an extensive low-CO region on a chromosome hundreds of megabases in length (see below) could be mediated by the centromere alone. The second aspect challenging the idea that regions of low CO rate in chromosome centres are driven by centromeres is that centromeres are not necessarily located in the physical centre of chromosomes. Hence, if the centromere was a major broad-scale determinant of the CO distribution, we would expect bias in CO rate towards chromosome peripheries to be restricted to chromosomes harbouring the centromeres near their centre. We assessed this prediction qualitatively by comparing the distribution of CO among species with different overall chromosome morphologies, as defined by their relative centromere position. This analysis revealed that species exhibiting exclusively acro- or telocentric chromosomes—that is, having centromeres located close to one chromosome end—still display reduced CO rates across the chromosome centre (or the centre of the longer chromosome arm) (Figure 2, left column; the pattern in species with metacentric chromosomes is shown in Figure S2). Moreover, some species with holocentric chromosomes, hence lacking a single well-defined centromeric domain, show the same broad-scale trend. Similar insights emerged from the comparison of different chromosome morphologies within species (Figure 2, right column; Figure S2). Collectively, these observations in no way challenge that the centromere influences the CO landscape, but show that the centromere alone fails to provide a universal explanation for the general broad-scale reduction in CO rate in chromosome centres seen across taxa.

### 3.4 | The distribution of CO is predicted by chromosome length

As a next step, we explored if the broad-scale distribution of CO was related to the length of chromosomes. For this, we quantified the relative elevation in CO rate in the chromosome peripheries by our CO periphery-bias statistic, and related this statistic to chromosome length. Pooling all species as data points in a single analysis revealed a clear association: organism lacking a marked reduction in the CO rate in chromosome centres (i.e., exhibiting CO periphery-bias around one) were those displaying short chromosomes, and the CO distribution became increasingly periphery-biased as chromosome length increased (Figure 3a; Spearman's rank correlation: $r_S = 0.86$, 95% CI: 0.74–0.93). This association also held when analysing animals and plants separately (animals: $r_S = 0.79$, 95% CI: 0.52–0.93; plants: $r_S = 0.87$, 95% CI: 0.68–0.95). A clear relationship between chromosome length and CO periphery-bias also emerged *within* species: the correlation between these two variables among chromosomes was almost consistently positive, and often strongly so, in both animals and plants (Figure 3b).

In combination, these analyses make clear that the magnitude of periphery-bias in CO rate is a function of the length of a chromosome. Organisms lacking a pronounced reduction in CO rate in chromosome centres are those having short chromosomes, typically below some 20 Mb. This includes species such as *Arabidopsis thaliana*, some social insects (honeybee, bumblebee) and, importantly, all fungi in our data set (the CO distribution along a representative chromosome from each of three species with short chromosomes is shown in Figure S3, left). Fungi are known to generally have short chromosomes (Cervelatti, Ferreira-Nozawa, Aquino-Ferreira, Fachin, & Martinez-Rossi, 2004), and this may well be the simple reason why our analysis of this group indicates a CO distribution qualitatively different from that seen in the other kingdoms (Figure 1). By contrast, the species in our data set exhibiting very long chromosomes, including wheat, maize, pepper, sunflower and several mammals, generally have CO restricted to short peripheral chromosome regions separated by a vast CO desert (three examples are shown in Figure S3, right). Based on these observations, it is tempting to propose a simple conceptual model in which CO occurs preferentially within a characteristic distance from the chromosome tips, and the total length of a chromosome then determines the physical extent of the central low-CO region (Figure 4). As suggested by Figure 3a, this characteristic distance may often be within some 10 Mb (see also

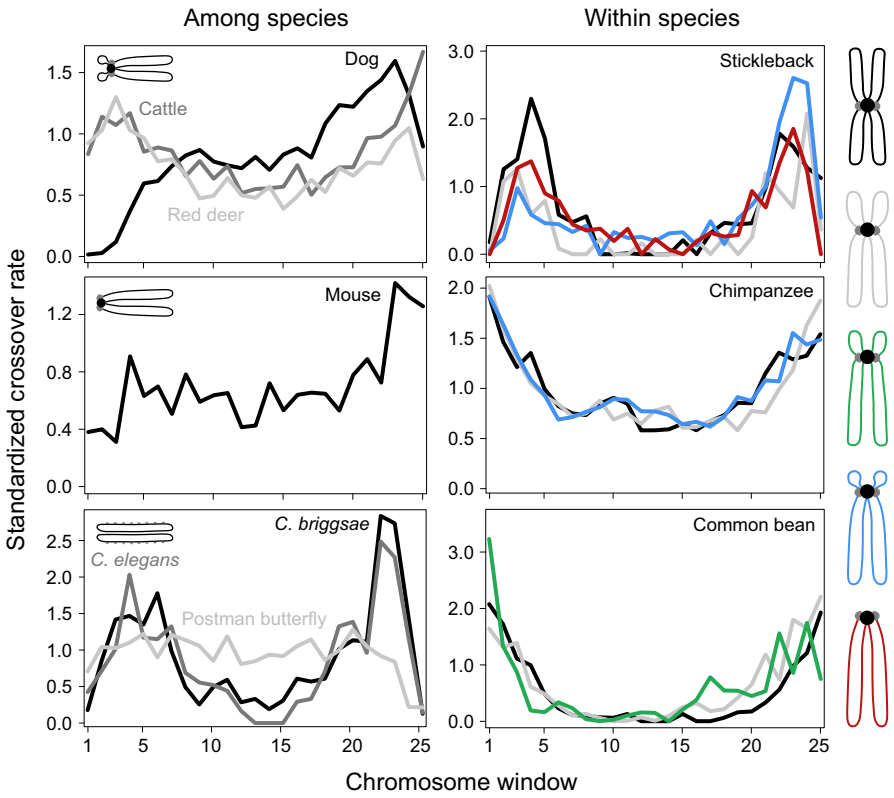


**FIGURE 2** Centromere position does not explain the widely observed broad-scale reduction in CO rate around the centre of chromosomes. The left column shows average CO rate profiles for species with uniform chromosome morphologies. From top to bottom, these are acrocentric, telocentric and holocentric chromosomes. The right column shows CO rate profiles for three exemplary species with variable chromosome morphologies. The colour coding refers to the chromosome morphology schematics, ordered from top to bottom by increasingly peripheral centromere position: metacentric in black, submetacentric in grey, subtelocentric in green, acrocentric in blue and telocentric in red. In each species, the profiles represent averages across at least three chromosomes for a given morphology. For both averaging and plotting, chromosomes were always oriented such that the shorter chromosome arm was on the left. In the chromosome schematics, the constriction separating the chromosome arms is shown in black and the kinetochore(s) in grey. CO rates and chromosome lengths were standardized for comparability as in Figure 1. Additional evidence from further species is presented in Figure S2

Johnston, Berenos, Slate, & Pemberton, 2016; Pratto et al., 2014; Roesti et al., 2013; Smeds, Mugal, Qvarnstrom, & Ellegren, 2016). According to this view, short chromosomes consist primarily of high-CO periphery. Before we evaluate the plausibility of this model in the light of evidence from investigations of the mechanisms governing meiosis, we consider a prediction regarding the genome-wide CO rate implicit in this model.

## 3.5 | Peripheral CO causes a negative association between average CO rate and chromosome length

The above conceptual model predicts that genomes consisting of short chromosomes, and hence mainly peripheral chromosome regions exhibiting a high CO rate, should show higher overall (i.e., genome-wide) CO rates than genomes consisting of long chromosomes with physically extensive centres of low CO rate. This prediction was confirmed: among species, we found a striking negative, nonlinear association between the average CO rate of chromosomes (or, equivalently, cumulative cM/Mb across the entire genome) and median chromosome length (Figure 5a, left panel, all species pooled; $r_S = -0.92$, 95% CI: −0.95 to −0.83). Extreme CO rates occurred in the species with the smallest chromosomes, including the two fungus species available for this specific analysis. A similar relationship emerged when analysing animals ($r_S = -0.90$, 95% CI: −0.96 to −0.77) and plants ($r_S = -0.84$, 95% CI: −0.94 to −0.60) separately. Interestingly, this relationship could be approximated by making the simplified assumption of a universal genetic map length of 50 cM per chromosome, corresponding to a single CO per chromosome and meiosis, and dividing this standard genetic map length by different physical chromosome lengths covering the range of median chromosome lengths observed in our organisms (Figure 5a, right panel). Chromosome length thus emerges as a remarkably strong predictor of the genome-wide CO rate among species, challenging the recent suggestion (Stapley, Feulner, Johnston, Santure, & Smadja, 2017) that features of genome architecture are relatively unimportant determinants of broad-scale CO rate variation among eukaryotes. Our insights from the analysis among species were further reinforced by relating CO rate to chromosome length *within* species. In both animals and plants, the correlation between these two variables was generally strongly negative among chromosomes (Figure 5b; the

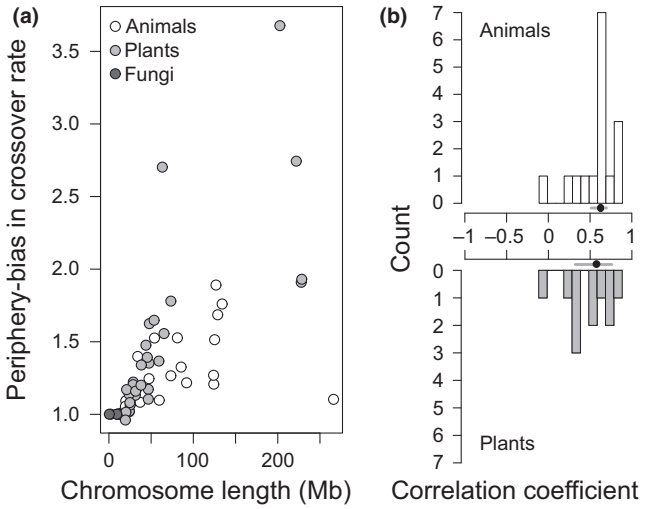


**FIGURE 3** The strength to which the CO rate is biased towards the chromosome peripheries is related to chromosome length. (a) Strength of periphery-bias in CO rate plotted against chromosome length, using species means as data points (colour-coded by kingdom). (b) Distribution of the strength of the correlation between CO periphery-bias and chromosome length within animal and plant species ($N$ = 16 and 11). A positive coefficient indicates that in a given species, the CO rate becomes more strongly biased towards the chromosome tips as chromosome length increases. The dots and error bars next to the $X$-axis show the median correlation coefficient and the associated 95% bootstrap CI for each kingdom

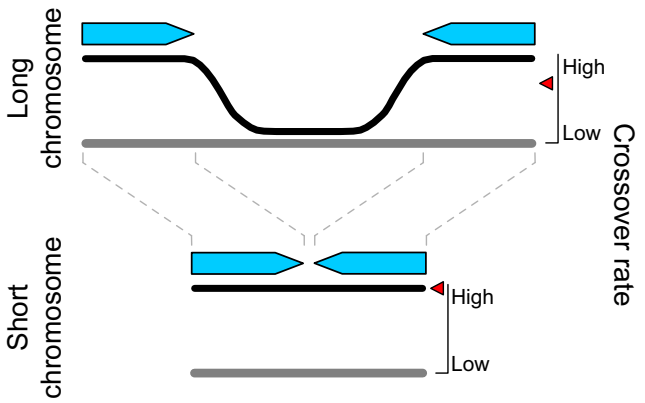


**FIGURE 4** A simple conceptual model for the broad-scale CO distribution in which the probability of CO along chromosomes (grey bars) is high only within a characteristic distance from the chromosome tips (blue arrows). On a long chromosome, these regions are separated, thus producing a region of low CO rate (black curve) in the chromosome's centre. On a short chromosome, by contrast, the probability of CO and hence the observed CO distribution is relatively homogeneous. Consequently, the average CO rate of a chromosome (red triangles) is a function of its length

distribution of correlation coefficients was not visualized for fungi because only two species were available, but both species also showed a negative coefficient; see also Backström et al., 2010; Giraut et al., 2011; International Human Genome Sequencing Consortium 2001; Jensen-Seaman et al., 2004; Johnston, Huisman, Ellis, & Pemberton, 2017; Kaback, Guacci, Barber, & Mahon, 1992; Roesti et al., 2013; Smeds et al., 2016; Tortereau et al., 2012).

Taken together, these analyses suggest that the genome-wide CO rate in eukaryotes is strongly determined by the relative proportion of the genome having a high rate of CO, that is, the proportion of peripheral DNA. For a given genome size, an organism may thus achieve a higher rate of CO—and thus stronger reshuffling of genetic variation—by distributing its total DNA among a greater number of smaller chromosomes. In the animal kingdom, particularly high genome-wide CO rates have been reported from social hymenopteran insects (Sirviö et al., 2006; Wilfert, Gadau, & Schmid-Hempel, 2007), with 37 cM/Mb in the honey bee (Beye et al., 2006; Liu et al., 2015; Solignac, Mougel, Vautrin, Monnerot, & Cornuet, 2007), 14 cM/Mb in *Pogonomyrmex* ants (Sirviö, Pamilo, Johnson, Page, & Gadau, 2011a), 9.7 cM/Mb in the common wasp (Sirviö, Johnston, Wenseleers, & Pamilo, 2011b) and 8.7 cM/Mb in the bumblebee (Liu et al., 2017). The evolutionary reason for this high average CO rate is not well understood, but perhaps reflects the need for rapid adaptation to fast-evolving pathogens to which social insects seem particularly strongly exposed, or for compensating the sex-limited recombination associated with haplo-diploid sex determination (Sirviö et al., 2006; Wilfert et al., 2007). However, these CO rates do not appear exceptionally high when taking heterogeneity in CO along chromosomes into account: species exhibiting a very low genome-wide CO rate (e.g., sunflower, wheat: 0.3 and 1.1 cM/Mb) reach similarly high CO rates as social insects when averaging exclusively over the terminal 5 Mb on either side of each chromosome (14.9 and 9.3 cM/Mb; see also Roesti et al., 2013; Pratto et al., 2014)—that is, when considering a total chromosome segment approximating median chromosome length in the honeybee (10.7 Mb) or bumblebee (14.5 Mb). Hence, a key feature of CO distinguishing some social insect species from other animals is that their genomes are split into many short chromosomes (Wilfert et al., 2007) lacking extensive central regions with a low CO rate. The same likely applies to fungi, a group also exhibiting very high genome-wide recombination rates and short chromosomes (Awadalla, 2003; Cervelatti et al., 2004; Stapley et al., 2017; Wilfert et al., 2007). Like social insects, many fungi also interact with other organisms as pathogens or through symbiosis, and have limited opportunity for recombination due to extensive haploid life phases, both of which may have selected for a high CO rate across their genomes. These considerations highlight the limited information conveyed by estimates of the average, genome-wide CO rate. Understanding to which extent genetic variation is shuffled by CO requires knowledge about the actual distribution of the CO rate within and among chromosomes.

### 3.6 | What causes the high CO rate in chromosome peripheries?

We have argued that a conceptual model in which CO happens mainly within some distance from the chromosome tips, irrespective of total chromosome length, helps explain associations between the average CO rate, the distribution of CO and chromosome length. Is

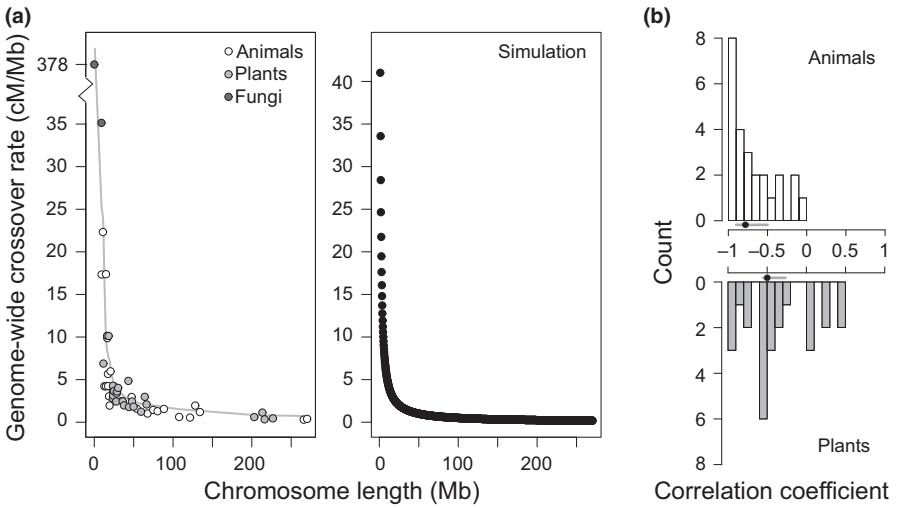


**FIGURE 5** The average CO rate is related to chromosome length. (a) The left panel displays the average genome-wide CO rate against median chromosome length, using species as data points (colour-coded by kingdom; only species for which genetic map length was available were considered, $N = 52$). The light grey curve shows a nonparametric fit (loess; moving average with bandwidth of 0.5) to the data pooled across the organismal kingdoms. The *Y*-axis is broken to allow for an extreme value. The right panel shows the corresponding relationship as simulated across the empirically observed chromosome length range based on the assumption of a universal single CO per chromosome and meiosis (50 cM genetic map length). The empirical chromosome length range was sampled at 1000 evenly spaced points. (b) Distribution of the strength of the correlation between the chromosome-wide CO rate and chromosome length within animal and plant species ($N = 25$ in both kingdoms). A negative correlation coefficient indicates that in a given species, long chromosomes exhibit a lower CO rate than short chromosomes. The dots and error bars next to the *X*-axis show the median correlation coefficient and the associated 95% bootstrap CI for each kingdom

there any mechanistic evidence in support of such a model? Indeed, an elegant explanation for periphery-bias in CO rate is related to the choreography of chromosomes and the spatio-temporal sequence of recombination initiation during meiosis. Higher eukaryotes generally share a phase in the early stages of meiosis during which the telomeres (i.e., the chromosome tips) aggregate at the nuclear membrane, while the chromosome centres remain closer to the nucleus' centre (Harper, Golubovskaya, & Cande, 2004; Naranjo & Corredor, 2008; Scherthan et al., 1996; Zickler & Kleckner, 2016). This stage, often referred to as the "meiotic bouquet" (Scherthan, 2001), is followed by rapid chromosome oscillations during which the chromosomes alternately disperse and aggregate (Klutstein & Cooper, 2014). This movement is again coordinated by the telomeres, which remain in contact with the nuclear membrane. The function of the bouquet and the oscillations remains incompletely understood, but very likely they enable homology search and the pairing of chromosomes (Bass et al., 2000; Chacon, Delivani, & Tolic, 2016; Curtis, Lukaszewski, & Chrzastek, 1991; Ding, Yamamoto, Haraguchi, & Hiraoka, 2004; Gerton & Hawley, 2005; Lee, Conrad, & Dresser, 2012; Lefrancois, Rockmill, Xie, Roeder, & Snyder, 2016; Page & Hawley, 2003). Intriguingly, these telomere-guided processes may also influence the location of CO along chromosomes: evidence from several organisms suggests that synapsis, that is, the establishment of a physical connection between homologous chromosomes, and associated DNA double-strand breaks required for CO are initiated from the chromosome tips, and that the repair of these breaks as CO is more likely in the chromosome peripheries than the centres (Anderson & Stack, 2005; Bass et al., 2000; Brown et al., 2005; Croft & Jones, 1989; Higgins, Osman, Jones, & Franklin, 2014; Klutstein & Cooper, 2014; Lukaszewski, 1997; Pratto et al., 2014; Viera, Santos, & Rufas, 2009; Xiang, Miller, Ross, Alvarado, & Hawley, 2014). The telomere-guided initiation of chromosome homology search and recombination could thus be part of the explanation why CO occurs primarily towards the chromosome peripheries (Scherthan et al., 1996; Zickler & Kleckner, 2016).

Another potentially important aspect is crossover interference, that is, the inhibition of additional CO in the vicinity of an existing CO along a chromosome (Muller, 1916; Sturtevant, 1915). This is suggested by sexual dimorphism in the distribution of CO: remarkably consistently across species, the enrichment of CO near the telomeres is more pronounced in the male than the female sex (Broman, Murray, Sheffield, White, & Weber, 1998; Cox et al., 2009; Giraut et al., 2011; Johnston et al., 2016, 2017; Lien et al., 2011; Ma et al., 2015; Smeds et al., 2016). Interestingly, the sexes also appear to differ in the structural organization of meiotic chromosomes, with the paired homologous chromosomes being less condensed in oocytes than spermatocytes (Tease & Hulten, 2004). If CO interference operates at the same spatial (i.e., μm, not base pairs) scale in both sexes, CO interference will therefore extend over a shorter base pair distance in females than males (Kochakpour & Moens, 2008; Petkov, Broman, Szatkiewicz, & Paigen, 2007). Consequently, male CO may be strongly limited to the chromosome tips where the first obligate CO occurs, whereas in females, additional CO may occur along the chromosomes, thus leading to a more homogeneous distribution of CO and an elevated overall CO count in females. Evaluating these ideas will require a more complete mechanistic understanding of meiosis based on experimental evidence from a wide variety of organismal systems.

### 3.7 | Implications of broad-scale heterogeneity in CO rate for evolutionary genomics

So far, we have demonstrated predictable broad-scale heterogeneity in CO rate along chromosomes, but what is the significance of this variation to evolutionary genomic theory and empirical analysis? A pivotal aspect of the CO rate is that it determines the physical scale of linked selection within a genome: allele frequency shifts driven by natural selection on a given locus extend relatively deeply into the locus' nonselected chromosomal neighbourhood when the locus is situated in a low-CO region, but decay over a shorter physical scale when the locus resides in a high-CO region (Maynard Smith & Haigh, 1974). Such linked selection has received distinct names in different evolutionary contexts, including "background selection" when the selected polymorphisms arise from new deleterious mutation (Charlesworth, Morgan, & Charlesworth, 1993; Hudson & Kaplan, 1995; Nordborg, Charlesworth, & Charlesworth, 1996); "genetic draft" when the polymorphisms arise from new beneficial mutations (Gillespie, 2000); and "gene flow barrier" when the polymorphisms arise from genetic exchange between populations under divergent selection (Aeschbacher, Selby, Willis, & Coop, 2017; Barton, 1979; Barton & Bengtsson, 1986; Berner & Roesti, 2017; Feder & Nosil, 2010; Roesti et al., 2014). These processes differ in detail. For instance, background selection is considered inevitable and ubiquitous because the majority of mutations are generally considered deleterious (Lynch et al., 1999). However, although plausibly occurring more rarely, new *beneficial* alleles arising from mutation will rise from initially low frequency, causing more intense selection than low-frequency deleterious mutations (Cutter & Payseur, 2013). Also, both background selection and genetic draft rely on new mutations and therefore have little impact on short time scales (Burri, 2017). By contrast, gene flow barriers can emerge rapidly by selection on standing genetic variation, although they require some level of genetic exchange between diverging populations (Berner & Roesti, 2017; see also Samuk et al., 2017). Despite these nuances, the different forms of linked selection can be housed under a single conceptual roof because they are all similarly affected by the CO rate. Importantly, natural selection implies a reduction in effective population size and hence elevated stochasticity in the transmission of genetic variation across generations (genetic drift) at a locus. By modifying the physical scale of linked selection around a locus, the CO rate thus influences the strength of drift in a genome region, and hence, the level of genetic diversity maintained within populations and of genetic differentiation among populations (Charlesworth, 1998; Cutter & Payseur, 2013; Nachman & Payseur, 2012).

Combined with the widespread broad-scale reduction in CO rate in chromosome centres relatively to chromosome peripheries, the above theory on linked selection predicts that populations should commonly harbour relatively low levels of genetic variation in chromosome centres, and that comparisons between populations should find relatively elevated genetic differentiation in chromosome centres (Figure 6). Genome-wide marker-based studies indeed support this prediction (Burri et al., 2015; Carneiro et al., 2014; Dutoit et al., 2017; Gante et al., 2016; Roesti et al., 2012, 2013; Samuk et al., 2017; Tine et al., 2014). However, elucidating the details in the underlying linked selection will often be difficult. The reason is that background selection and genetic draft are notoriously hard to disentangle (Comeron, 2017; Cutter & Payseur, 2013). Moreover, gene flow between population and species can persist over long time spans (Berner & Salzburger, 2015), so that selection on new mutations and selection against immigrant alleles (gene flow barrier) may shape patterns in genetic variation jointly (Aeschbacher et al., 2017). Only when divergence between populations is so recent that a substantial contribution from selection on new mutations can be ruled out, broad-scale patterns in genetic diversity and population differentiation can be ascribed to linked selection caused by heterogeneity along chromosomes in the strength of gene flow barriers.

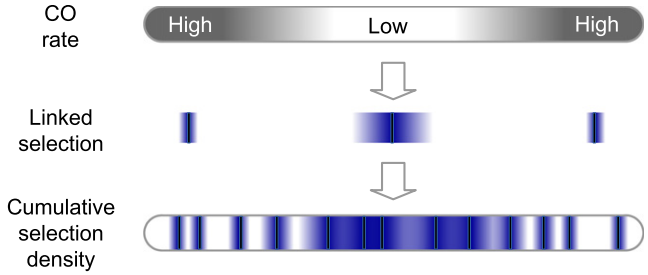


**FIGURE 6** Relationship between heterogeneous CO rate and selection density along a chromosome. If the CO rate is reduced in the chromosome centre relative to the peripheries (top), selection on a locus (shown as black vertical bar) in the centre will cause linked selection to extend deeper into the locus' chromosomal neighbourhood than in the peripheries (middle; the strength of linked selection is visualized by the blue shade). Consequently, selection at many loci—due to continued mutation over long timescales and/or to gene flow between populations in selectively different habitats—will generate a relatively elevated cumulative density of linked selection in the chromosome centre (bottom). This elevated selection density implies a reduction in effective population size, and hence stronger drift, in chromosome centres. Chromosome centres will therefore harbour less genetic variation within populations and exhibit elevated genetic differentiation among populations, relative to the peripheries

The above reflections make clear that heterogeneity in the distribution of CO across the genome is a key determinant of heterogeneity in the distribution of genetic variation within and between populations. Equally important, however, is the distribution of selective targets along chromosomes: if regions of low CO rate coincide with regions of low gene density, selection on new mutations or maladaptive immigrant alleles may not necessarily drive heterogeneity in diversity and differentiation across the genome (Aeschbacher et al., 2017; Cutter & Payseur, 2013; Payseur & Nachman, 2002). The reason is that the wider physical extent of linked selection in a low-CO region is counterbalanced by a reduced probability of selection to target this region in the first place. Understanding how heterogeneous CO rate modifies the consequences of selection across the genome thus benefits from knowledge about the broad-scale distribution of selection targets along chromosomes. This motivated our analysis of the density of genes along chromosomes, considering the subset of species in our data set for which annotated

genomes were available. We found no indication of systematic broad-scale heterogeneity in gene density along chromosomes in animals or fungi (Figure 7a): in these groups, genes appear distributed relatively evenly along chromosomes (noting that sample size for fungi was low). In striking contrast, a clear pattern emerged in plants: on average, gene density proved ~3.5 times higher towards the chromosome peripheries than in the chromosome centres. These findings were confirmed by examining the correlations between gene density and CO rate within each species: in animals, the correlation coefficients peaked around zero, whereas in plants, the correlations were consistently positive and mostly very strong (Figure 7b). Our investigation thus highlights a peculiarity of plant genomes: genes tend to be located in chromosome regions crossing over relatively frequently (see also Gaut, Wright, Rizzon, Dvorak, & Anderson, 2007; Mezard, 2006; Schnable, Hsia, & Nikolau, 1998). As recombination is a potent mechanism of DNA loss counteracting the proliferation of transposable elements, it is possible that in many plant species, chromosome centres with a low CO rate have developed into gene-poor regions through the accumulation of repetitive DNA (Bennetzen, 2000; Puchta, 2005; Hawkins, Grover, & Wendel, 2008; Schubert & Vu, 2016; see also Nam & Ellegren, 2012; Kapusta, Suh, & Feschotte, 2017). Nevertheless, the heterogeneity in CO rate across plant genomes on average still exceeds the heterogeneity in gene density, although not as strongly as in animals (dotted lines in Figure 7a). The consequences of natural selection should thus tend to be more profound in chromosome centres than in the peripheries in both taxonomic groups, but particularly strongly so in animals.

### 3.8 | Empirical demonstration of analytical challenges of broad-scale heterogeneity in CO rate to evolutionary genomics

As described above, a relatively reduced CO rate across chromosome centres in combination with selection can drive systematically elevated population differentiation in chromosome centres. This has serious but insufficiently recognized implications to analytical approaches commonly employed in evolutionary genomics. Importantly, the identification of so-called outlier loci—that is, genetic markers showing particularly strong population differentiation relative to the genome-wide background level and hence considered footprints of divergent selection—can be misleading when using outlier detection approaches ignoring heterogeneity in the CO landscape. Such outliers will tend to be overrepresented in genome regions of low CO rate (Noor & Bennett 2009; Berner & Roesti, 2017) because loci under selection and their selectively neutral chromosomal neighbourhood can reach stronger population differentiation through cumulative linked selection in low-CO regions (Roesti et al., 2012, 2013; Aeschbacher et al., 2017; see Roesti et al., 2012 for a pragmatic approach to adjust marker data for such broad-scale heterogeneity in differentiation). A related inferential problem can arise in investigations of genomic parallelism in evolution. The extent to which repeated adaptive phenotypic divergence in multiple population pairs occurs by responses to divergent selection in the same genes is an important question in evolutionary genomics (Arendt & Reznick, 2008; Bailey, Blanquart, Bataillon, & Kassen, 2017). Popular approaches to addressing this question include evaluating the

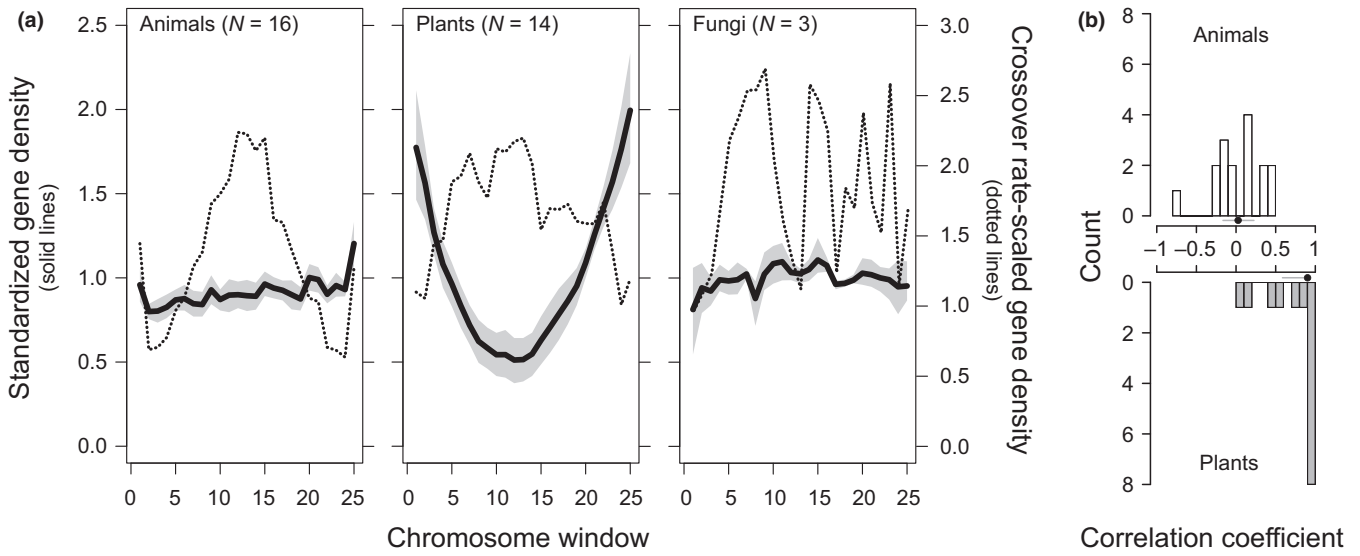


**FIGURE 7** (a) Broad-scale distribution of gene density along chromosomes in each kingdom (sample sizes in parentheses). Following the conventions from Figure 1, each chromosome was scaled to unit length and divided into 25 windows, gene density was standardized by the average value across windows for each chromosome, and window-specific median values across all chromosomes were calculated within each species. The solid black lines, referring to the left *Y*-axis scale, are mean values across species, with 95% bootstrap CIs shown as grey bands. The dotted lines, referring to the right *Y*-axis scale, represent standardized gene density divided by standardized CO rate (see Figure 1) for each window and hence express the density of genes along chromosomes relative to the CO rate. (b) Distribution of the coefficients of correlation between gene density and CO rate within species, shown separately for animals and plants. The correlations were calculated based on chromosome window-specific median values for both variables. The dots and error bars next to the X-axis show the median correlation coefficient and the associated 95% bootstrap CI for each kingdom

proportion of high-differentiation outliers (individual markers, or chromosome windows) shared among multiple population comparisons, or to examine whether a correlation in the magnitude of differentiation in markers or chromosome windows exists among multiple population comparisons. Shared outliers and/or correlated differentiation are then often interpreted as indication that divergent natural selection has targeted the same genes in multiple population pairs, and hence as evidence of parallel evolution at the molecular level. However, such analyses are frequently performed with low physical marker resolution (recent examples: Egger, Roesti, Böhne, Roth, & Salzburger, 2017; Perreault-Payette et al., 2017; Ravinet et al., 2016; Raeymaekers et al., 2017; Rougemont et al., 2017; Stuart et al., 2017; Trucchi, Frajman, Haverkamp, Schönswetter, & Paun, 2017). Consequently, single markers are highly unlikely to coincide with polymorphisms under direct selection. Shared population differentiation captured by such marker or chromosome window data may thus primarily mirror common patterns in cumulative linked selection density shaped by a shared broad-scale CO landscape, thus precluding reliable conclusions about (non)parallelism in the specific targets of divergent selection (Berner & Roesti, 2017). This view is particularly plausible when shared patterns in genome-wide differentiation emerge across lineages separated for a long time (Burri et al., 2015; Dutoit et al., 2017; Renaut, Owens, & Rieseberg, 2014; Van Doren et al., 2017; see also Hobolth, Dutheil, Hawks, Schierup, & Mailund, 2011). We emphasize that studies using high-density markers (e.g., as obtained by whole-genome sequencing) are not immune to such confounding if marker-specific differentiation data are averaged across large chromosome windows.

To illustrate these conceptual issues with empirical data, we re-analysed relatively low-resolution SNP data from two ecologically distinct population comparisons of threespine stickleback fish (Roesti et al., 2012, 2014), that is, a lake–stream and a marine–freshwater population pair. Chromosome window-based profiles of population differentiation revealed strikingly elevated differentiation in chromosome centres, a pattern evident in *both ecologically different* population comparisons (Figure 8a). As a consequence, the magnitude of window-specific differentiation was correlated between the two

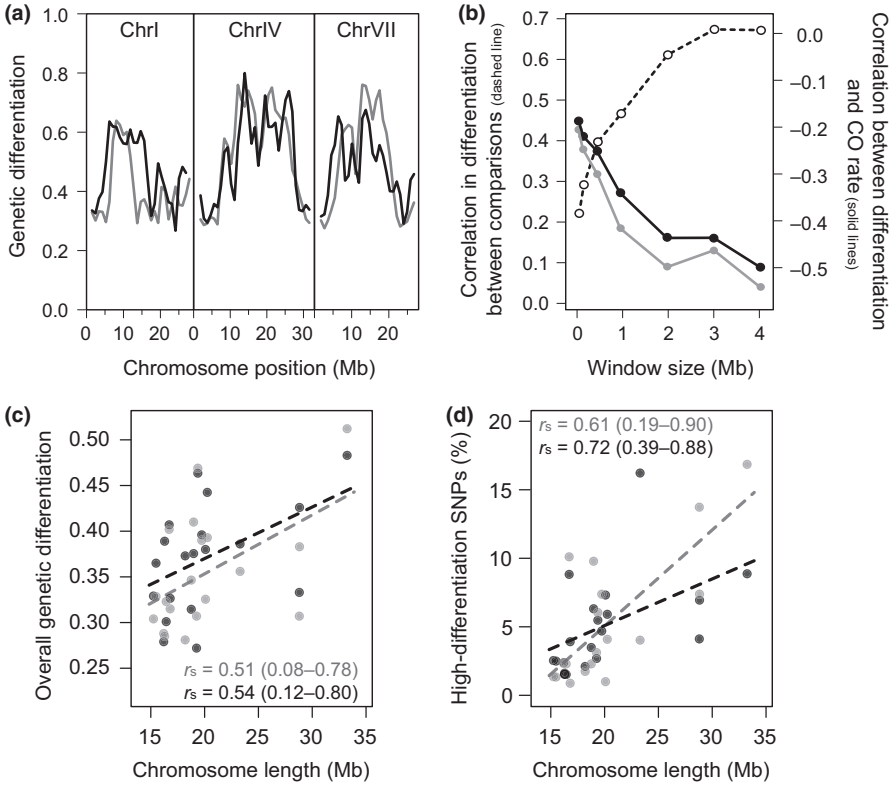


**FIGURE 8** (a) Genetic differentiation (quantified by the absolute allele frequency difference, AFD) in a lake–stream (black) and a marine–freshwater (grey; same colour coding used throughout the graphic) stickleback population comparison along the three largest chromosomes exhibiting a particularly pronounced reduction in CO rate around their centres (Roesti et al., 2013). The profiles show mean differentiation across all SNPs for nonoverlapping chromosome windows of 1 Mb. (b) The strength of the correlation between the lake–stream and the marine–freshwater population comparison in the magnitude of differentiation across chromosome windows increases with increasing window size (0.1–4 Mb), shown by the dashed line referring to the left *Y*-axis. Likewise, the negative association between average population differentiation and CO rate across chromosome windows increases within each population comparison as window size increases (solid lines, referring to the right *Y*-axis). (c) and (d) illustrate that both the magnitude of overall differentiation (median AFD) and the relative proportion of SNPs displaying high differentiation (upper 5% of the genome-wide AFD distribution) are correlated to the length of chromosomes in each population comparison (Spearman correlations and their 95% bootstrap CIs are given in each box). Note that the proportion of high-differentiation SNPs is adjusted for the total number of SNPs along a focal chromosome, and hence, a high value indicates a relative excess of strongly differentiated SNPs on a chromosome

population pairs, increasingly strongly so when averaging differentiation values across SNPs for increasingly large physical windows (Figure 8b). A naive interpretation of this association would be that selection has targeted the same genes in both population comparisons. A more parsimonious explanation, however, is that irrespective of the precise targets of selection and the underlying ecological context in each population pair, gene flow barriers have driven shared patterns of broad-scale neutral differentiation across the genome. Indeed, stickleback exhibit strongly reduced CO rates in chromosome centres (Roesti et al., 2013; Glazer, Killingbeck, Mitros, Rokhsar, & Miller, 2015; see also Figure 2), and adaptive divergence in both lake–stream and marine–freshwater stickleback systems is well known to occur in the face of gene flow and to involve selection on a large number of genes (Berner et al., 2009; Hagen, 1967; Jones, Brown, Pemberton, & Braithwaite, 2006; Jones et al., 2012; Lescak et al., 2015; Roesti et al., 2014, 2015; Terekhanova et al., 2014)—conditions facilitating the emergence of heterogeneous differentiation through variation in the strength of gene flow barriers along chromosomes (Berner & Roesti, 2017). (Note that divergence in both population pairs is postglacial and hence too recent for mutation-based linked selection to significantly influence differentiation profiles.) Accordingly, both population comparisons also exhibited a negative genome-wide correlation between population differentiation and CO rate, a relationship increasing in strength with decreasing analytical resolution (Figure 8b). Moreover, in line with the general observation that the relative reduction in CO rate around chromosome centres increases with chromosome length, we found stronger overall population differentiation and a relative excess of high-differentiation SNPs (i.e., adjusted for total SNP number on a chromosome) on longer chromosomes (Figure 8c, d). In diverging stickleback populations, chromosome length thus appears to influence genome-wide heterogeneity in the opportunity for genetic exchange between populations by determining heterogeneity in the strength of gene flow barriers along chromosomes.

The above analytical challenges emphasize the value of two resources in evolutionary genomics: the first is a chromosome-level genome assembly. Combined with genetic map data, an assembly allows characterizing the CO landscape and recognizing broad-scale trends in diversity and differentiation, thus potentially revealing an interaction between the distribution of CO and selection density. The second key resource is a high marker resolution. Inference about targets of selection—a major goal in many evolutionary genomic studies—requires an analytical resolution much finer than the broad scale of the patterns in genetic variation driven by heterogeneity in CO-mediated selection density. We argue that in the light of widespread variation in CO rate along chromosomes, these two aspects deserve more weight when designing evolutionary genomic investigations.

## 4 | CONCLUSION

Our synthesis of the distribution of crossovers in 62 species reveals a taxonomically widespread trend for CO to occur primarily towards the peripheries of chromosomes. This distribution of CO rate is closely linked to the physical length of chromosomes and strongly influences the genome-wide average CO rate. Although we can rule out the centromere as major driver of this chromosome-scale heterogeneity in CO rate, substantial progress in recombination research will be needed to identify the underlying mechanistic determinants, and to allow assessing to what extent these determinants are shared among organisms. Given the strong impact of the CO landscape on the consequences of natural selection to genetic diversity within and between populations, quantifying and embracing heterogeneity in CO rate should become a standard element of analytical approaches and their interpretation in evolutionary genomics.

## ACKNOWLEDGEMENTS

We kindly thank all researchers who have made this synthesis possible by making primary data available; Scott Hawley and Danny Miller for discussion; Gleb Ebert for helping extract data; Reto Burri and two anonymous reviewers for valuable feedback; Louis Bernatchez for inviting this review. DB was supported financially by the Swiss National Science Foundation (SNF; grant 31003A_165826) and the University of Basel. MR was supported by the SNF and a Janggen-Pöhn fellowship.

## CONFLICT OF INTEREST

The authors declare no competing financial interests.

## DATA ACCESSIBILITY

Table S1 and Figures S1–S3 can be found online in Appendix S1. Supporting data are provided as Appendices S2, S3 and S4. The raw data sets are available on Dryad (https://doi.org/10.5061/dryad.p1j7n43).

## AUTHOR CONTRIBUTIONS

Q.H. contributed to literature search, led data extraction, and performed data analysis; T.G.L. contributed to study design, literature search and data extraction, performed data analysis and contributed to manuscript writing; M.R. contributed to study design, literature search and data analysis; D.B. designed and supervised the study, contributed to literature search and data extraction, developed analytical tools, performed data analysis and wrote the paper with feedback from all co-authors.

## ORCID

*Telma G. Laurentino* http://orcid.org/0000-0001-7879-5251
*Marius Roesti* http://orcid.org/0000-0002-7408-4804

## REFERENCES

Aeschbacher, S., Selby, J. P., Willis, J. H., & Coop, G. (2017). Population–genomic inference of the strength and timing of selection against gene flow. *Proceedings of the National Academy of Sciences of the*

*United States of America*, *114*, 7061–7066. https://doi.org/10.1073/pnas.1616755114

Akhunov, E. D., Goodyear, A. W., Geng, S., Qi, L.-L., Echalier, B., Gill, B. S., … Dvorak, J. (2003). The organization and rate of evolution of wheat genomes are correlated with recombination rates along chromosome arms. *Genome Research*, *13*, 753–763. https://doi.org/10.1101/gr.808603

Allshire, R. C., & Karpen, G. H. (2008). Epigenetic regulation of centromeric chromatin: Old dogs, new tricks? *Nature Review Genetics*, *9*, 923–937. https://doi.org/10.1038/nrg2466

Anderson, L. K., & Stack, S. M. (2005). Recombination nodules in plants. *Cytogenetic and Genome Research*, *109*, 198–204. https://doi.org/10.1159/000082400

Arendt, J., & Reznick, D. (2008). Convergence and parallelism reconsidered: What have we learned about the genetics of adaptation? *Trends in Ecology and Evolution*, *23*, 26–32. https://doi.org/10.1016/j.tree.2007.09.011

Argout, X., Salse, J., Aury, J. M., Guiltinan, M. J., Droc, G., Gouzy, J., … Lanaud, C. (2011). The genome of *Theobroma cacao*. *Nature Genetics*, *43*, 101–108. https://doi.org/10.1038/ng.736

Argyris, J. M., Ruiz-Herrera, A., Madriz-Masis, P., Sanseverino, W., Morata, J., Pujol, M., … Garcia-Mas, J. (2015). Use of targeted SNP selection for an improved anchoring of the melon (*Cucumis melo* L.) scaffold genome assembly. *BMC Genomics*, *16*, 4. https://doi.org/10.1186/s12864-014-1196-3

Arias, J. A., Keehan, M., Fisher, P., Coppieters, W., & Spelman, R. (2009). A high density linkage map of the bovine genome. *BMC Genetics*, *10*, 18. https://doi.org/10.1186/1471-2156-10-18

Auton, A., Fledel-Alon, A., Pfeifer, S., Venn, O., Segurel, L., Street, T., … McVean, G. (2012). A fine-scale chimpanzee genetic map from population sequencing. *Science*, *336*, 193–198. https://doi.org/10.1126/science.1216872

Awadalla, P. (2003). The evolutionary genomics of pathogen recombination. *Nature Review Genetics*, *4*, 50–60. https://doi.org/10.1038/nrg964

Backström, N., Forstmeier, W., Schielzeth, H., Mellenius, H., Nam, K., Bolund, E., … Ellegren, H. (2010). The recombination landscape of the zebra finch *Taeniopygia guttata* genome. *Genome Research*, *20*, 485–495. https://doi.org/10.1101/gr.101410.109

Bailey, S. F., Blanquart, F., Bataillon, T., & Kassen, R. (2017). What drives parallel evolution? How population size and mutational variation contribute to repeated evolution. *BioEssays*, *39*, 1–9.

Barton, N. H. (1979). Gene flow past a cline. *Heredity*, *43*, 333–339. https://doi.org/10.1038/hdy.1979.86

Barton, N. H. (1995). A general model for the evolution of recombination. *Genetics Research*, *65*, 123–144. https://doi.org/10.1017/S0016672300033140

Barton, N., & Bengtsson, B. O. (1986). The barrier to genetic exchange between hybridizing populations. *Heredity*, *57*, 357–376. https://doi.org/10.1038/hdy.1986.135

Barton, N. H., & Otto, S. P. (2005). Evolution of recombination due to random drift. *Genetics*, *169*, 2353–2370. https://doi.org/10.1534/genetics.104.032821

Bass, H. W., Riera-Lizarazu, O., Ananiev, E. V., Bordoli, S. J., Rines, H. W., Phillips, R. L., … Cande, W. Z. (2000). Evidence for the coincident initiation of homolog pairing and synapsis during the telomere-clustering (bouquet) stage of meiotic prophase. *Journal of Cell Science*, *113*, 1033–1042.

Baudat, F., Imai, Y., & de Massy, B. (2013). Meiotic recombination in mammals: Localization and regulation. *Nature Review Genetics*, *14*, 794–806. https://doi.org/10.1038/nrg3573

Bauer, E., Falque, M., Walter, H., Bauland, C., Camisan, C., Campo, L., … Schön, C.-C. (2013). Intraspecific variation of recombination rate in maize. *Genome Biology*, *14*, 1–17.

Beadle, G. W. (1932). A possible influence of the spindle fibre on crossing-over in *Drosophila*. *Proceedings of the National Academy of Sciences of the United States of America*, *18*, 160–165. https://doi.org/10.1073/pnas.18.2.160

Bekele, W. A., Wieckhorst, S., Friedt, W., & Snowdon, R. J. (2013). High-throughput genomics in sorghum: From whole-genome resequencing to a SNP screening array. *Plant Biotechnology Journal*, *11*, 1112–1125. https://doi.org/10.1111/pbi.12106

Bennetzen, J. L. (2000). Transposable element contributions to plant gene and genome evolution. *Plant Molecular Biology*, *42*, 251–269. https://doi.org/10.1023/A:1006344508454

Berner, D., Adams, D. C., Grandchamp, A.-C., & Hendry, A. P. (2008). Natural selection drives patterns of lake-stream divergence in stickleback foraging morphology. *Journal of Evolutionary Biology*, *21*, 1653–1665. https://doi.org/10.1111/j.1420-9101.2008.01583.x

Berner, D., Grandchamp, A.-C., & Hendry, A. P. (2009). Variable progress toward ecological speciation in parapatry: Stickleback across eight lake-stream transitions. *Evolution*, *63*, 1740–1753. https://doi.org/10.1111/j.1558-5646.2009.00665.x

Berner, D., & Roesti, M. (2017). Genomics of adaptive divergence with chromosome-scale heterogeneity in crossover rate. *Molecular Ecology*, *26*, 6351–6369. https://doi.org/10.1111/mec.14373

Berner, D., & Salzburger, W. (2015). The genomics of organismal diversification illuminated by adaptive radiations. *Trends in Genetics*, *31*, 491–499. https://doi.org/10.1016/j.tig.2015.07.002

Beye, M., Gattermeier, I., Hasselmann, M., Gempe, T., Schioett, M., Baines, J. F., … Page, R. E. (2006). Exceptionally high levels of recombination across the honey bee genome. *Genome Research*, *16*, 1339–1344. https://doi.org/10.1101/gr.5680406

Bhakta, M. S., Jones, V. A., & Vallejos, C. E. (2015). Punctuated distribution of recombination hotspots and demarcation of pericentromeric regions in *Phaseolus vulgaris* L. *PLoS ONE*, *10*, e0116822. https://doi.org/10.1371/journal.pone.0116822

Blankers, T., Oh, K. P., Bombarely, A., & Shaw, K. L. (2017). The genomic architecture of a rapid island radiation: Mapping chromosomal rearrangements and recombination rate variation in *Laupala*. *bioRxiv*. https://doi.org/10.1101/160952

Bradley, K. M., Breyer, J. P., Melville, D. B., Broman, K. W., Knapik, E. W., & Smith, J. R. (2011). An SNP-based linkage map for zebrafish reveals sex determination loci. *G3: Genes, Genomes, Genetics*, *1*, 3–9. https://doi.org/10.1534/g3.111.000190

Broman, K. W., Murray, J. C., Sheffield, V. C., White, R. L., & Weber, J. L. (1998). Comprehensive human genetic maps: Individual and sex-specific variation in recombination. *The American Journal of Human Genetics*, *63*, 861–869. https://doi.org/10.1086/302011

Brown, P. W., Judis, L. A., Chan, E. R., Schwartz, S., Seftel, A., Thomas, A., & Hassold, T. J. (2005). Meiotic synapsis proceeds from a limited number of subtelomeric sites in the human male. *American Journal of Human Genetics*, *77*, 556–566. https://doi.org/10.1086/468188

Burri, R. (2017). Interpreting differentiation landscapes in the light of long-term linked selection. *Evolution Letters*, *1*, 118–131. https://doi.org/10.1002/evl3.14

Burri, R., Nater, A., Kawakami, T., Mugal, C. F., Olason, P. I., Smeds, L., … Ellegren, H. (2015). Linked selection and recombination rate variation drive the evolution of the genomic landscape of differentiation across the speciation continuum of *Ficedula* flycatchers. *Genome Research*, *25*, 1656–1665. https://doi.org/10.1101/gr.196485.115

Burt, A. (2000). Sex, recombination, & the efficacy of selection – was Weismann right? *Evolution*, *54*, 337–351.

Burt, A., & Bell, G. (1987). Mammalian chiasma frequencies as a test of two theories of recombination. *Nature*, *326*, 803–805.

Carneiro, M., Albert, F. W., Afonso, S., Pereira, R. J., Burbano, H., Campos, R., … Ferrand, N. (2014). The genomic architecture of population divergence between subspecies of the European rabbit. *PLoS Genetics*, *10*, e1003519. https://doi.org/10.1371/journal.pgen.1003519

Cervelatti, E. P., Ferreira-Nozawa, M. S., Aquino-Ferreira, R., Fachin, A. L., & Martinez-Rossi, N. M. (2004). Electrophoretic molecular karyotype of the dermatophyte *Trichophyton rubrum*. *Genetics and Molecular Biology*, *27*, 99–102. https://doi.org/10.1590/S1415-47572004000100016

Chacon, M. R., Delivani, P., & Tolic, I. M. (2016). Meiotic nuclear oscillations are necessary to avoid excessive chromosome associations. *Cell Reports*, *17*, 1632–1645. https://doi.org/10.1016/j.celrep.2016.10.014

Charlesworth, B. (1998). Measures of divergence between populations and the effect of forces that reduce variability. *Molecular Biology and Evolution*, *15*, 538–543. https://doi.org/10.1093/oxfordjournals.molbev.a025953

Charlesworth, B., Morgan, M. T., & Charlesworth, D. (1993). The effect of deleterious mutations on neutral molecular variation. *Genetics*, *134*, 1289–1303.

Cherry, J. M., Hong, E. L., Amundsen, C., Balakrishnan, R., Binkley, G., Chan, E. T., … Wong, E. D. (2012). *Saccharomyces* genome database: The genomics resource of budding yeast. *Nucleic Acids Research*, *40*, D700–D705. https://doi.org/10.1093/nar/gkr1029

Choi, K., & Henderson, I. R. (2015). Meiotic recombination hotspots – a comparative view. *The Plant Journal*, *83*, 52–61. https://doi.org/10.1111/tpj.12870

Comeron, J. M. (2017). Background selection as null hypothesis in population genomics: Insights and challenges from *Drosophila* studies. *Proceedings of the Royal Society B*, *372*, 20160471.

Comeron, J. M., Ratnappan, R., & Bailin, S. (2012). The many landscapes of recombination in *Drosophila melanogaster*. *PLoS Genetics*, *8*, e1002905. https://doi.org/10.1371/journal.pgen.1002905

Cox, A., Ackert-Bicknell, C. L., Dumont, B. L., Ding, Y., Bell, J. T., Brockmann, G. A., … Broman, K. A. (2009). A new standard genetic map for the laboratory mouse. *Genetics*, *182*, 1335–1344. https://doi.org/10.1534/genetics.109.105486

Croft, J. A., & Jones, G. H. (1989). Meiosis in *Mesostoma ehrenbergii ehrenbergii*. IV. Recombination nodules in spermatocytes and a test of the correspondence of late recombination nodules and chiasmata. *Genetics*, *121*, 255–262.

Croll, D., Lendenmann, M. H., Stewart, E., & McDonald, B. A. (2015). The impact of recombination hotspots on genome evolution of a fungal plant pathogen. *Genetics*, *201*, 1213–1228. https://doi.org/10.1534/genetics.115.180968

Curtis, C. A., Lukaszewski, A. J., & Chrzastek, M. (1991). Metaphase I pairing of deficient chromosomes and genetic mapping of deficiency breakpoints in common wheat. *Genome*, *34*, 553–560. https://doi.org/10.1139/g91-085

Cutter, A. D., & Payseur, B. A. (2013). Genomic signatures of selection at linked sites: Unifying the disparity among species. *Nature Review Genetics*, *14*, 262–274. https://doi.org/10.1038/nrg3425

Da Ines, O., Gallego, M. E., & White, C. I. (2014). Recombination-independent mechanisms and pairing of homologous chromosomes during meiosis in plants. *Molecular Plant*, *7*, 492–501. https://doi.org/10.1093/mp/sst172

Daccord, N., Celton, J. M., Linsmith, G., Becker, C., Choisne, N., Schijlen, E., … Bucher, E. (2017). High-quality de novo assembly of the apple genome and methylome dynamics of early fruit development. *Nature Genetics*, *49*, 1099–1106. https://doi.org/10.1038/ng.3886

Davey, J. W., Chouteau, M., Barker, S. L., Maroja, L., Baxter, S. W., Simpson, F., … Jiggins, C. D. (2016). Major improvements to the *Heliconius melpomene* genome assembly used to confirm 10 chromosome fusion events in 6 million years of butterfly evolution. *G3: Genes, Genomes, Genetics*, *6*, 695–708. https://doi.org/10.1534/g3.115.023655

Deokar, A. A., Ramsay, L., Sharpe, A. G., Diapari, M., Sindhu, A., Bett, K., … Tar'an, B. (2014). Genome wide SNP identification in chickpea for use in development of a high density genetic map and improvement of chickpea reference genome assembly. *BMC Genomics*, *15*, 708. https://doi.org/10.1186/1471-2164-15-708

Dernburg, A. F. (2001). Here, there, & everywhere: Kinetochore function on holocentric chromosomes. *Journal of Cell Biology*, *153*, F33–F38. https://doi.org/10.1083/jcb.153.6.F33

Ding, D. Q., Yamamoto, A., Haraguchi, T., & Hiraoka, Y. (2004). Dynamics of homologous chromosome pairing during meiotic prophase in fission yeast. *Developmental Cell*, *6*, 329–341. https://doi.org/10.1016/S1534-5807(04)00059-0

Dohm, J. C., Lange, C., Holtgrawe, D., Sorensen, T. R., Borchardt, D., Schulz, B., … Himmelbauer, H. (2012). Palaeohexaploid ancestry for Caryophyllales inferred from extensive gene-based physical and genetic mapping of the sugar beet genome (*Beta vulgaris*). *The Plant Journal*, *70*, 528–540. https://doi.org/10.1111/j.1365-313X.2011.04898.x

Dohm, J. C., Minoche, A. E., Holtgrawe, D., Capella-Gutierrez, S., Zakrzewski, F., Tafer, H., … Himmelbauer, H. (2014). The genome of the recently domesticated crop plant sugar beet (*Beta vulgaris*). *Nature*, *505*, 546–549. https://doi.org/10.1038/nature12817

Dukić, M., Berner, D., Roesti, M., Haag, C. R., & Ebert, D. (2016). A high-density genetic map reveals variation in recombination rate across the genome of *Daphnia magna*. *BMC Genetics*, *17*, 137.

Dutoit, L., Vijay, N., Mugal, C. F., Bossu, C. M., Burri, R., Wolf, J. B. W., & Ellegren, H. (2017). Covariation in levels of nucleotide diversity in homologous regions of the avian genome long after completion of lineage sorting. *Proceedings of the Royal Society B*, *284*, 20162756. https://doi.org/10.1098/rspb.2016.2756

Egger, B., Roesti, M., Böhne, A., Roth, O., & Salzburger, W. (2017). Demography and genome divergence of lake and stream populations of an East African cichlid fish. *Molecular Ecology*, *26*, 5016–5030. https://doi.org/10.1111/mec.14248

Ellermeier, C., Higuchi, E. C., Phadnis, N., Holm, L., Geelhood, J. L., Thon, G., & Smith, G. R. (2010). RNAi and heterochromatin repress centromeric meiotic recombination. *Proceedings of the National Academy of Sciences of the United States of America*, *107*, 8701–8705. https://doi.org/10.1073/pnas.0914160107

Endelman, J. B., & Jansky, S. H. (2016). Genetic mapping with an inbred line-derived F2 population in potato. *Theoretical and Applied Genetics*, *129*, 935–943. https://doi.org/10.1007/s00122-016-2673-7

Feder, J. L., & Nosil, P. (2010). The efficacy of divergence hitchhiking in generating genomic islands during ecological speciation. *Evolution*, *64*, 1729–1747. https://doi.org/10.1111/j.1558-5646.2009.00943.x

Felsenstein, J. (1974). The evolutionary advantage of recombination. *Genetics*, *78*, 737–756.

Fisher, R. A. (1930). *The genetical theory of natural selection*. Oxford, UK: Oxford University. https://doi.org/10.5962/bhl.title.27468

Gante, H. F., Matschiner, M., Malmstrom, M., Jakobsen, K. S., Jentoft, S., & Salzburger, W. (2016). Genomics of speciation and introgression in Princess cichlid fishes from Lake Tanganyika. *Molecular Ecology*, *25*, 6143–6161. https://doi.org/10.1111/mec.13767

Gardner, K. A., Wittern, L. M., & Mackay, I. J. (2016). A highly recombined, high-density, eight-founder wheat MAGIC map reveals extensive segregation distortion and genomic locations of introgression segments. *Plant Biotechnology Journal*, *14*, 1406–1417. https://doi.org/10.1111/pbi.12504

Gaut, B. S., Wright, S. I., Rizzon, C., Dvorak, J., & Anderson, L. K. (2007). Recombination: An underappreciated factor in the evolution of plant genomes. *Nature Review Genetics*, *8*, 77–84. https://doi.org/10.1038/nrg1970

Gerton, J. L., & Hawley, R. S. (2005). Homologous chromosome interactions in meiosis: Diversity amidst conservation. *Nature Review Genetics*, *6*, 477–487. https://doi.org/10.1038/nrg1614

Gillespie, J. H. (2000). Genetic drift in an infinite population: The pseudohitchhiking model. *Genetics*, *155*, 909–919.

Giraut, L., Falque, M., Drouaud, J., Pereira, L., Martin, O. C., & Mezard, C. (2011). Genome-wide crossover distribution in *Arabidopsis thaliana* meiosis reveals sex-specific patterns along chromosomes. *PLoS Genetics*, *7*, e1002354. https://doi.org/10.1371/journal.pgen.1002354

Glazer, A. M., Killingbeck, E. E., Mitros, T., Rokhsar, D. S., & Miller, C. T. (2015). Genome assembly improvement and mapping convergently evolved skeletal traits in sticklebacks with genotyping-by-sequencing. *G3: Genes, Genomes, Genetics*, *5*, 1463–1472. https://doi.org/10.1534/g3.115.017905

Groenen, M. A., Wahlberg, P., Foglio, M., Cheng, H. H., Megens, H. J., Crooijmans, R. P., … Andersson, L. (2009). A high-density SNP-based linkage map of the chicken genome reveals sequence features correlated with recombination rate. *Genome Research*, *19*, 510–519.

Hagen, D. W. (1967). Isolating mechanisms in threespine sticklebacks (*Gasterosteus*). *Journal of the Fisheries Research Board of Canada*, *24*, 1637–1692. https://doi.org/10.1139/f67-138

Harper, L., Golubovskaya, I., & Cande, W. Z. (2004). A bouquet of chromosomes. *Journal of Cell Science*, *117*, 4025–4032. https://doi.org/10.1242/jcs.01363

Hartfield, M., & Otto, S. P. (2011). Recombination and hitchhiking of deleterious alleles. *Evolution*, *65*, 2421–2434. https://doi.org/10.1111/j.1558-5646.2011.01311.x

Harushima, Y., Yano, M., Shomura, P., Sato, M., Shimano, T., Kuboki, Y., … Sasaki, T. (1998). A high–density rice genetic linkage map with 2275 markers using a single F–2 population. *Genetics*, *148*, 479–494.

Hassold, T., & Hunt, P. (2001). To err (meiotically) is human: The genesis of human aneuploidy. *Nature Review Genetics*, *2*, 280–291. https://doi.org/10.1038/35066065

Hawkins, J. S., Grover, C. E., & Wendel, J. F. (2008). Repeated big bangs and the expanding universe: Directionality in plant genome size evolution. *Plant Science*, *174*, 557–562. https://doi.org/10.1016/j.plantsci.2008.03.015

Higgins, J. D., Osman, K., Jones, G. H., & Franklin, F. C. H. (2014). Factors underlying restricted crossover localization in barley meiosis. *Annual Review of Genetics*, *48*, 29–47. https://doi.org/10.1146/annurev-genet-120213-092509

Hill, T., Ashrafi, H., Chin-Wo, S. R., Stoffel, K., Truco, M.-J., Kozik, A., … Van Deynze, A. (2015). Ultra-high density, transcript-based genetic maps of pepper define recombination in the genome and synteny among related species. *G3: Genes, Genomes, Genetics*, *5*, 2341–2355. https://doi.org/10.1534/g3.115.020040

Hill, W. G., & Robertson, A. (1966). Effect of linkage on limits to artificial selection. *Genetics Research*, *8*, 269. https://doi.org/10.1017/S0016672300010156

Hobolth, A., Dutheil, J. Y., Hawks, J., Schierup, M. H., & Mailund, T. (2011). Incomplete lineage sorting patterns among human, chimpanzee, and orangutan suggest recent orangutan speciation and widespread selection. *Genome Research*, *21*, 349–356. https://doi.org/10.1101/gr.114751.110

Holeski, L. M., Monnahan, P., Koseva, B., McCool, N., Lindroth, R. L., & Kelly, J. K. (2014). A high-resolution genetic map of yellow monkeyflower identifies chemical defense QTLs and recombination rate variation. *G3: Genes, Genomes, Genetics*, *4*, 813–821. https://doi.org/10.1534/g3.113.010124

Houle, D. (1992). Comparing evolvability and variability of quantitative traits. *Genetics*, *130*, 195–204.

Huang, L., Yang, Y., Zhang, F., & Cao, J. (2017). A genome-wide SNP-based genetic map and QTL mapping for agronomic traits in Chinese cabbage. *Scientific Reports*, *7*, 46305. https://doi.org/10.1038/srep46305

Hudson, R. R., & Kaplan, N. L. (1995). Deleterious background selection with recombination. *Genetics*, *141*, 1605–1617.

Hunter, N. (2007). Meiotic recombination. In A. Aguilera, & R. Rothstein (Eds.), *Molecular genetics of recombination* (pp. 381–442). Berlin, Germany: Springer. https://doi.org/10.1007/978-3-540-71021-9

Huo, N., Garvin, D. F., You, F. M., McMahon, S., Luo, M. C., Gu, Y. Q., … Vogel, J. P. (2011). Comparison of a high-density genetic linkage map to genome features in the model grass *Brachypodium distachyon*. *Theoretical and Applied Genetics*, *123*, 455–464. https://doi.org/10.1007/s00122-011-1598-4

International Human Genome Sequencing Consortium (2001). Initial sequencing and analysis of the human genome. *Nature*, *409*, 860–921.

International Peach Genome Initiative, Verde, I., Abbott, A. G., Scalabrin, S., Jung, S., Shu, S., … Rokhsar, D. S. (2013). The high-quality draft genome of peach (*Prunus persica*) identifies unique patterns of genetic diversity, domestication and genome evolution. *Nature Genetics*, *45*, 487–494. https://doi.org/10.1038/ng.2586

Jensen-Seaman, M. I., Furey, T. S., Payseur, B. A., Lu, Y. T., Roskin, K. M., Chen, C. F., … Jacob, H. J. (2004). Comparative recombination rates in the rat, mouse, & human genomes. *Genome Research*, *14*, 528–538. https://doi.org/10.1101/gr.1970304

Johnston, S. E., Berenos, C., Slate, J., & Pemberton, J. M. (2016). Conserved genetic architecture underlying individual recombination rate variation in a wild population of soay sheep (*Ovis aries*). *Genetics*, *203*, 583–598. https://doi.org/10.1534/genetics.115.185553

Johnston, S. E., Huisman, J., Ellis, P. A., & Pemberton, J. M. (2017). A high density linkage map reveals sexual dimorphism in recombination landscapes in red deer (*Cervus elaphus*). *G3: Genes, Genomes, Genetics*, *7*, 2859–2870. https://doi.org/10.1534/g3.117.044198

Jones, F. C., Brown, C., Pemberton, J. M., & Braithwaite, V. A. (2006). Reproductive isolation in a threespine stickleback hybrid zone. *Journal of Evolutionary Biology*, *19*, 1531–1544. https://doi.org/10.1111/j.1420-9101.2006.01122.x

Jones, F. C., Chan, Y. F., Schmutz, J., Grimwood, J., Brady, S. D., Southwick, A. M., … Kingsley, D. M. (2012). A genome-wide SNP genotyping array reveals patterns of global and repeated species–pair divergence in sticklebacks. *Current Biology*, *22*, 83–90. https://doi.org/10.1016/j.cub.2011.11.045

Juneja, P., Osei-Poku, J., Ho, Y. S., Ariani, C. V., Palmer, W. J., Pain, A., & Jiggins, F. M. (2014). Assembly of the genome of the disease vector *Aedes aegypti* onto a genetic linkage map allows mapping of genes affecting disease transmission. *PLoS Neglected Tropical Diseases*, *8*, e2652. https://doi.org/10.1371/journal.pntd.0002652

Kaback, D. B., Guacci, V., Barber, D., & Mahon, J. W. (1992). Chromosome size-dependent control of meiotic recombination. *Science*, *256*, 228–232. https://doi.org/10.1126/science.1566070

Kapusta, A., Suh, A., & Feschotte, C. (2017). Dynamics of genome size evolution in birds and mammals. *Proceedings of the National Academy of Sciences of the United States of America*, *114*, E1460–E1469. https://doi.org/10.1073/pnas.1616702114

Kawakami, T., Smeds, L., Backstrom, N., Husby, A., Qvarnstrom, A., Mugal, C. F., … Ellegren, H. (2014). A high-density linkage map enables a second-generation collared flycatcher genome assembly and reveals the patterns of avian recombination rate variation and chromosomal evolution. *Molecular Ecology*, *23*, 4035–4058. https://doi.org/10.1111/mec.12810

Kirkpatrick, M., & Barton, N. (2006). Chromosome inversions, local adaptation and speciation. *Genetics*, *173*, 419–434. https://doi.org/10.1534/genetics.105.047985

Klutstein, M., & Cooper, J. P. (2014). The chromosomal courtship dance – homolog pairing in early meiosis. *Current Opinion in Cell Biology*, *26*, 123–131. https://doi.org/10.1016/j.ceb.2013.12.004

Kochakpour, N., & Moens, P. B. (2008). Sex-specific crossover patterns in Zebrafish (*Danio rerio*). *Heredity*, *100*, 489–495. https://doi.org/10.1038/sj.hdy.6801091

Kondrashov, A. S. (1982). Selection against harmful mutations in large sexual and asexual populations. *Genetics Research*, *40*, 325–332. https://doi.org/10.1017/S0016672300019194

Lambie, E. J., & Roeder, G. S. (1986). Repression of meiotic crossing over by a centromere (CEN3) in *Saccharomyces cerevisiae*. *Genetics*, *114*, 769–789.

Laurent, B., Palaiokostas, C., Spataro, C., Moinard, M., Zehraoui, E., Houston, R. D., & Foulongne-Oriol, M. (2017). High-resolution mapping of

the recombination landscape of the phytopathogen *Fusarium graminearum* suggests two-speed genome evolution. *Molecular Plant Pathology*, https://doi.org/10.1111/mpp.12524

Lee, C. Y., Conrad, M. N., & Dresser, M. E. (2012). Meiotic chromosome pairing is promoted by telomere-led chromosome movements independent of bouquet formation. *PLoS Genetics*, *8*(5), e1002730. https://doi.org/10.1371/journal.pgen.1002730

Lefrancois, P., Rockmill, B., Xie, P. X., Roeder, G. S., & Snyder, M. (2016). Multiple pairwise analysis of non-homologous centromere coupling reveals preferential chromosome size-dependent interactions and a role for bouquet formation in establishing the interaction pattern. *PLoS Genetics*, *12*(10), e1006347. https://doi.org/10.1371/journal.pgen.1006347

Lescak, E. A., Bassham, S. L., Catchen, J., Gelmond, O., Sherbick, M. L., von Hippel, F. A., & Cresko, W. A. (2015). Evolution of stickleback in 50 years on earthquake-uplifted islands. *Proceedings of the National Academy of Sciences of the United States of America*, *112*, E7204–E7212. https://doi.org/10.1073/pnas.1512020112

Levan, A., Fredga, K., & Sandberg, A. A. (1964). Nomenclature for centromeric position on chromosomes. *Hereditas*, *52*, 201–220.

Li, G., Hillier, L. W., Grahn, R. A., Zimin, A. V., David, V. A., Menotti-Raymond, M., … William, J. M. (2016). A high-resolution SNP array-based linkage map anchors a new domestic cat draft genome assembly and provides detailed patterns of recombination. *G3: Genes, Genomes, Genetics*, *6*, 1607–1616. https://doi.org/10.1534/g3.116.028746

Lichten, M., & Goldman, A. S. H. (1995). Meiotic recombination hotspots. *Annual Review of Genetics*, *29*, 423–444. https://doi.org/10.1146/annurev.ge.29.120195.002231

Lien, S., Gidskehaug, L., Moen, T., Hayes, B. J., Berg, P. R., Davidson, W. S., … Kent, M. P. (2011). A dense SNP-based linkage map of Atlantic salmon (*Salmo salar*) reveals extended chromosome homeologies and striking differences in sex-specific recombination patterns. *BMC Genomics*, *12*, 615. https://doi.org/10.1186/1471-2164-12-615

Liu, H., Jia, Y., Sun, X., Tian, D., Hurst, L. D., & Yang, S. (2017). Direct determination of the mutation rate in the bumblebee reveals evidence for weak recombination-associated mutation and an approximate rate constancy in insects. *Molecular Biology and Evolution*, *34*, 119–130. https://doi.org/10.1093/molbev/msw226

Liu, Z., Liu, S., Yao, J., Bao, L., Zhang, J., Li, Y., … Waldbieser, G. C. (2016). The channel catfish genome sequence provides insights into the evolution of scale formation in teleosts. *Nature Communications*, *7*, 11757. https://doi.org/10.1038/ncomms11757

Liu, H., Zhang, X., Huang, J., Chen, J. Q., Tian, D., Hurst, L. D., & Yang, S. (2015). Causes and consequences of crossing-over evidenced via a high-resolution recombinational landscape of the honey bee. *Genome Biology*, *16*, 15. https://doi.org/10.1186/s13059-014-0566-0

Lukaszewski, A. J. (1997). The development and meiotic behavior of asymmetrical isochromosomes in wheat. *Genetics*, *145*, 1155–1160.

Luo, M. C., You, F. M., Li, P., Wang, J. R., Zhu, T., Dandekar, A. M., … Dvorak, J. (2015). Synteny analysis in Rosids with a walnut physical map reveals slow genome evolution in long-lived woody perennials. *BMC Genomics*, *16*, 707. https://doi.org/10.1186/s12864-015-1906-5

Lynch, M., Blanchard, J., Houle, D., Kibota, T., Schultz, S., Vassilieva, L., & Willis, J. (1999). Perspective: Spontaneous deleterious mutation. *Evolution*, *53*, 645–663. https://doi.org/10.1111/j.1558-5646.1999.tb05361.x

Ma, L., O'Connell, J. R., VanRaden, P. M., Shen, B., Padhi, A., Sun, C., … Wiggans, G. R. (2015). Cattle sex-specific recombination and genetic control from a large pedigree analysis. *PLoS Genetics*, *11*, e1005387. https://doi.org/10.1371/journal.pgen.1005387

Mahtani, M. M., & Willard, H. F. (1998). Physical and genetic mapping of the human X chromosome centromere: Repression of recombination. *Genome Research*, *8*, 100–110. https://doi.org/10.1101/gr.8.2.100

Malik, H. S., & Henikoff, S. (2009). Major evolutionary transitions in centromere complexity. *Cell*, *138*, 1067–1082. https://doi.org/10.1016/j.cell.2009.08.036

Manly, B. F. J. (2007). *Randomization, bootstrap and Monte Carlo methods in biology*, 3rd edn. Boca Raton, FL: Chapman & Hall.

Mather, K. (1938). Crossing-over. *Biological Reviews*, *13*, 252–292. https://doi.org/10.1111/j.1469-185X.1938.tb00516.x

Maynard Smith, J., & Haigh, J. (1974). Hitch-hiking effect of a favorable gene. *Genetics Research*, *23*, 23–35. https://doi.org/10.1017/S0016672300014634

McFarlane, R. J., & Humphrey, T. C. (2010). A role for recombination in centromere function. *Trends in Genetics*, *26*, 209–213. https://doi.org/10.1016/j.tig.2010.02.005

Melters, D. P., Paliulis, L. V., Korf, I. F., & Chan, S. W. L. (2012). Holocentric chromosomes: Convergent evolution, meiotic adaptations, & genomic analysis. *Chromosome Research*, *20*, 579–593. https://doi.org/10.1007/s10577-012-9292-1

Mezard, C. (2006). Meiotic recombination hotspots in plants. *Biochemical Society Transactions*, *34*, 531–534. https://doi.org/10.1042/BST0340531

Muller, H. J. (1916). The mechanism of crossing-over. *American Naturalist*, *50*, 193–221. https://doi.org/10.1086/279534

Muller, H. J. (1932). Some genetic aspects of sex. *American Naturalist*, *66*, 118–138. https://doi.org/10.1086/280418

Muñoz-Fuentes, V., Marcet-Ortega, M., Alkorta-Aranburu, G., Linde Forsberg, C., Morrell, J. M., Manzano-Piedras, E., … Vila, C. (2015). Strong artificial selection in domestic mammals did not result in an increased recombination rate. *Molecular Biology and Evolution*, *32*, 510–523. https://doi.org/10.1093/molbev/msu322

Nachman, M. W., & Churchill, G. A. (1996). Heterogeneity in rates of recombination across the mouse genome. *Genetics*, *142*, 537–548.

Nachman, M. W., & Payseur, B. A. (2012). Recombination rate variation and speciation: Theoretical predictions and empirical results from rabbits and mice. *Philosophical Transactions of the Royal Society B*, *367*, 409–421. https://doi.org/10.1098/rstb.2011.0249

Nam, K., & Ellegren, H. (2012). Recombination drives vertebrate genome contraction. *PLoS Genetics*, *8*(5), e1002680. https://doi.org/10.1371/journal.pgen.1002680

Naranjo, T., & Corredor, E. (2008). Nuclear architecture and chromosome dynamics in the search of the pairing partner in meiosis in plants. *Cytogenetic and Genome Research*, *120*, 320–330. https://doi.org/10.1159/000121081

Niehuis, O., Gibson, J. D., Rosenberg, M. S., Pannebakker, B. A., Koevoets, T., Judson, A. K., … Gadau, J. (2010). Recombination and its impact on the genome of the haplodiploid parasitoid wasp *Nasonia*. *PLoS ONE*, *5*, e8597. https://doi.org/10.1371/journal.pone.0008597

Noor, M. A. F., & Bennett, S. M. (2009). Islands of speciation or mirages in the desert? Examining the role of restricted recombination in maintaining species. *Heredity*, *103*, 439–444.

Nordborg, M., Charlesworth, B., & Charlesworth, D. (1996). The effect of recombination on background selection. *Genetics Research*, *67*, 159–174. https://doi.org/10.1017/S0016672300033619

Nunes, J. D. D., Liu, S. K., Pertille, F., Perazza, C. A., Villela, P. M. S., de Almeida-Val, V. M. F., … Coutinho, L. L. (2017). Large-scale SNP discovery and construction of a high-density genetic map of *Colossoma macropomum* through genotyping-by-sequencing. *Scientific Reports*, *7*, 46112. https://doi.org/10.1038/srep46112

Ortiz-Barrientos, D., Reiland, J., Hey, J., & Noor, M. A. F. (2002). Recombination and the divergence of hybridizing species. *Genetica*, *116*, 167–178. https://doi.org/10.1023/A:1021296829109

Otto, S. P., & Barton, N. H. (1997). The evolution of recombination: Removing the limits to natural selection. *Genetics*, *147*, 879–906.

Otto, S. P., & Barton, N. H. (2001). Selection for recombination in small populations. *Evolution*, *55*, 1921–1931. https://doi.org/10.1111/j.0014-3820.2001.tb01310.x

Page, S. L., & Hawley, R. S. (2003). Chromosome choreography: The meiotic ballet. *Science*, *301*, 785–789. https://doi.org/10.1126/science.1086605

Payseur, B. A., & Nachman, M. W. (2002). Gene density and human nucleotide polymorphism. *Molecular Biology and Evolution*, *19*, 336–340. https://doi.org/10.1093/oxfordjournals.molbev.a004086

Perreault-Payette, A., Muir, A. M., Goetz, F., Perrier, C., Normandeau, E., Sirois, P., & Bernatchez, L. (2017). Investigating the extent of parallelism in morphological and genomic divergence among lake trout ecotypes in Lake Superior. *Molecular Ecology*, *26*, 1477–1497. https://doi.org/10.1111/mec.14018

Petkov, P. M., Broman, K. W., Szatkiewicz, J. P., & Paigen, K. (2007). Crossover interference underlies sex differences in recombination rates. *Trends in Genetics*, *23*, 539–542. https://doi.org/10.1016/j.tig.2007.08.015

Pratto, F., Brick, K., Khil, P., Smagulova, F., Petukhova, G. V., & Camerini-Otero, R. D. (2014). Recombination initiation maps of individual human genomes. *Science*, *346*, 1256442. https://doi.org/10.1126/science.1256442

Puchta, H. (2005). The repair of double-strand breaks in plants: Mechanisms and consequences for genome evolution. *Journal of Experimental Botany*, *56*, 1–14.

R Core Team (2017). *R: A language and environment for statistical computing*. Vienna, Austria: R Foundation for Statistical Computing.

Raeymaekers, J. A. M., Chaturvedi, A., Hablützel, P. I., Verdonck, I., Hellemans, B., Maes, G. E., … Volckaert, F. A. M. (2017). Adaptive and non–adaptive divergence in a common landscape. *Nature Communications*, *8*, 267. https://doi.org/10.1038/s41467-017-00256-6

Rahn, M. I., & Solari, A. J. (1986). Recombination nodules in the oocytes of the chicken, *Gallus domesticus*. *Cytogenetic and Cell Genetics*, *43*, 187–193. https://doi.org/10.1159/000132319

Ravinet, M., Westram, A., Johannesson, K., Butlin, R., Andre, C., & Panova, M. (2016). Shared and nonshared genomic divergence in parallel ecotypes of *Littorina saxatilis* at a local scale. *Molecular Ecology*, *25*, 287–305. https://doi.org/10.1111/mec.13332

Rees, H., & Dale, P. J. (1974). Chiasmata and variability in *Lolium* and *Festuca* populations. *Chromosoma*, *47*, 335–351. https://doi.org/10.1007/BF00328866

Ren, Y., Zhao, H., Kou, Q., Jiang, J., Guo, S., Zhang, H., … Xu, Y. (2012). A high resolution genetic map anchoring scaffolds of the sequenced watermelon genome. *PLoS ONE*, *7*, e29453. https://doi.org/10.1371/journal.pone.0029453

Renaut, S., Grassa, C. J., Yeaman, S., Moyers, B. T., Lai, Z., Kane, N. C., … Rieseberg, L. H. (2013). Genomic islands of divergence are not affected by geography of speciation in sunflowers. *Nature Communications*, *4*, 1827. https://doi.org/10.1038/ncomms2833

Renaut, S., Owens, G. L., & Rieseberg, L. H. (2014). Shared selective pressure and local genomic landscape lead to repeatable patterns of genomic divergence in sunflowers. *Molecular Ecology*, *23*, 311–324. https://doi.org/10.1111/mec.12600

Rockman, M. V., & Kruglyak, L. (2009). Recombinational landscape and population genomics of *Caenorhabditis elegans*. *PLoS Genetics*, *5*, e1000419.

Roesti, M., Gavrilets, S., Hendry, A. P., Salzburger, W., & Berner, D. (2014). The genomic signature of parallel adaptation from shared genetic variation. *Molecular Ecology*, *23*, 3944–3956. https://doi.org/10.1111/mec.12720

Roesti, M., Hendry, A. P., Salzburger, W., & Berner, D. (2012). Genome divergence during evolutionary diversification as revealed in replicate lake-stream stickleback population pairs. *Molecular Ecology*, *21*, 2852–2862. https://doi.org/10.1111/j.1365-294X.2012.05509.x

Roesti, M., Kueng, B., Moser, D., & Berner, D. (2015). The genomics of ecological vicariance in threespine stickleback fish. *Nature Communications*, *6*, 8767. https://doi.org/10.1038/ncomms9767

Roesti, M., Moser, D., & Berner, D. (2013). Recombination in the threespine stickleback genome – patterns and consequences. *Molecular Ecology*, *22*, 3014–3027. https://doi.org/10.1111/mec.12322

Ross, J. A., Koboldt, D. C., Staisch, J. E., Chamberlin, H. M., Gupta, B. P., Miller, R. D., … Haag, E. S. (2011). Caenorhabditis briggsae recombinant inbred line genotypes reveal inter-strain incompatibility and the evolution of recombination. *PLoS Genetics*, *7*, e1002174. https://doi.org/10.1371/journal.pgen.1002174

Ross-Ibarra, J. (2004). The evolution of recombination under domestication: A test of two hypotheses. *American Naturalist*, *163*, 105–112. https://doi.org/10.1086/380606

Rougemont, Q., Gagnaire, P. A., Perrier, C., Genthon, C., Besnard, A. L., Launey, S., & Evanno, G. (2017). Inferring the demographic history underlying parallel genomic divergence among pairs of parasitic and nonparasitic lamprey ecotypes. *Molecular Ecology*, *26*, 142–162. https://doi.org/10.1111/mec.13664

Samuk, K., Owens, G. L., Delmore, K. E., Miller, S. E., Rennison, D. J., & Schluter, D. (2017). Gene flow and selection interact to promote adaptive divergence in regions of low recombination. *Molecular Ecology*, *17*, 4378–4390. https://doi.org/10.1111/mec.14226

Scherthan, H. (2001). A bouquet makes ends meet. *Nature Reviews Molecular Cell Biology*, *2*, 621–627. https://doi.org/10.1038/35085086

Scherthan, H., Weich, S., Schwegler, H., Heyting, C., Harle, M., & Cremer, T. (1996). Centromere and telomere movements during early meiotic prophase of mouse and man are associated with the onset of chromosome pairing. *Journal of Cell Biology*, *134*, 1109–1125. https://doi.org/10.1083/jcb.134.5.1109

Schmutz, J., Cannon, S. B., Schlueter, J., Ma, J., Mitros, T., Nelson, W., … Jackson, S. A. (2010). Genome sequence of the palaeopolyploid soybean. *Nature*, *463*, 178–183. https://doi.org/10.1038/nature08670

Schnable, P. S., Hsia, A. P., & Nikolau, B. J. (1998). Genetic recombination in plants. *Current Opinions in Plant Biology*, *1*, 123–129. https://doi.org/10.1016/S1369-5266(98)80013-7

Schubert, I., & Vu, G. T. H. (2016). Genome stability and evolution: Attempting a holistic view. *Trends Plant Sciences*, *21*, 749–757. https://doi.org/10.1016/j.tplants.2016.06.003

Sherman, J. D., & Stack, S. M. (1995). Two–dimensional spreads of synaptonemal complexes from solanaceous plants. VI. High-resolution recombination nodule map for tomato (*Lycopersicon esculentum*). *Genetics*, *141*, 683–708.

Shriver, M. D., Smith, M. W., Jin, L., Marcini, A., Akey, J. M., Deka, R., & Ferrell, R. E. (1997). Ethnic-affiliation estimation by use of population-specific DNA markers. *American Journal of Human Genetics*, *60*, 957–964.

Shulaev, V., Sargent, D. J., Crowhurst, R. N., Mockler, T. C., Folkerts, O., Delcher, A. L., … Folta, K. M. (2011). The genome of woodland strawberry (*Fragaria vesca*). *Nature Genetics*, *43*, 109–116. https://doi.org/10.1038/ng.740

Sim, S. B., & Geib, S. M. (2017). A chromosome-scale assembly of the *Bactrocera cucurbitae* genome provides insight to the genetic basis of white pupae. *G3: Genes, Genomes, Genetics*, *7*, 1927–1940.

Sirviö, A., Gadau, J., Rueppell, O., Lamatsch, D., Boomsma, J. J., Pamilo, P., & Page, R. E. (2006). High recombination frequency creates genotypic diversity in colonies of the leaf-cutting ant *Acromyrmex echinatior*. *Journal of Evolutionary Biology*, *19*, 1475–1485. https://doi.org/10.1111/j.1420-9101.2006.01131.x

Sirviö, A., Johnston, J. S., Wenseleers, T., & Pamilo, P. (2011b). A high recombination rate in eusocial Hymenoptera: Evidence from the common wasp *Vespula vulgaris*. *BMC Genetics*, *12*, 95. https://doi.org/10.1186/1471-2156-12-95

Sirviö, A., Pamilo, P., Johnson, R. A., Page, R. E. Jr, & Gadau, J. (2011a). Origin and evolution of the dependent lineages in the genetic caste determination system of *Pogonomyrmex* ants. *Evolution*, *65*, 869–884. https://doi.org/10.1111/j.1558-5646.2010.01170.x

Smeds, L., Mugal, C. F., Qvarnstrom, A., & Ellegren, H. (2016). High-resolution mapping of crossover and non-crossover recombination events by whole-genome re-sequencing of an avian pedigree. *PLoS Genetics*, *12*, e1006044. https://doi.org/10.1371/journal.pgen.1006044

Smith, K. N., & Nicolas, A. (1998). Recombination at work for meiosis. *Current Opinion in Genetics & Development*, *8*, 200–211. https://doi.org/10.1016/S0959-437X(98)80142-1

Solignac, M., Mougel, F., Vautrin, D., Monnerot, M., & Cornuet, J. M. (2007). A third-generation microsatellite–based linkage map of the honey bee, *Apis mellifera*, and its comparison with the sequence-based physical map. *Genome Biology*, *8*, R66. https://doi.org/10.1186/gb-2007-8-4-r66

Stapley, J., Feulner, P. G. D., Johnston, S. E., Santure, A. W., & Smadja, C. M. (2017). Variation in recombination frequency and distribution across eukaryotes: Patterns and processes. *Philosophical Transactions of the Royal Society B: Biological Sciences*, *372*, 20160455. https://doi.org/10.1098/rstb.2016.0455

Stuart, Y. E., Veen, T., Weber, J. N., Hanson, D., Ravinet, M., Lohman, B. K., … Bolnick, D. I. (2017). Contrasting effects of environment and genetics generate a continuum of parallel evolution. *Nature Ecology and Evolution*, *1*, 0158. https://doi.org/10.1038/s41559-017-0158

Sturtevant, A. H. (1915). The behavior of the chromosomes as studied through linkage. *Zeitschrift für indukive Abstammungs- und Vererbungslehre*, *13*, 234–287.

Talbert, P. B., & Henikoff, S. (2010). Centromeres convert but don't cross. *PLoS Biology*, *8*, e1000326.

Tease, C., & Hulten, M. A. (2004). Inter-sex variation in synaptonemal complex lengths largely determine the different recombination rates in male and female germ cells. *Cytogenetic and Genome Research*, *107*, 208–215. https://doi.org/10.1159/000080599

Terekhanova, N. V., Logacheva, M. D., Penin, A. A., Neretina, T. V., Barmintseva, A. E., Bazykin, G. A., … Mugue, N. S. (2014). Fast evolution from precast bricks: Genomics of young freshwater populations of threespine stickleback *Gasterosteus aculeatus*. *PLoS Genetics*, *10*, e1004696. https://doi.org/10.1371/journal.pgen.1004696

Tian, Z., Rizzon, C., Du, J., Zhu, L., Bennetzen, J. L., Jackson, S. A., … Ma, J. (2009). Do genetic recombination and gene density shape the pattern of DNA elimination in rice long terminal repeat retrotransposons? *Genome Research*, *19*, 2221–2230. https://doi.org/10.1101/gr.083899.108

Tine, M., Kuhl, H., Gagnaire, P.-N. D. A. S. H.-A., Louro, B., Desmarais, E., Martins, R. S. T., … Reinhardt, R. (2014). European sea bass genome and its variation provide insights into adaptation to euryhalinity and speciation. *Nature Communications*, *5*, 5770. https://doi.org/10.1038/ncomms6770

Tomato Genome Consortium (2012). The tomato genome sequence provides insights into fleshy fruit evolution. *Nature*, *485*, 635–641.

Tong, C., Li, H., Wang, Y., Li, X., Ou, J., Wang, D., … Shi, J. (2016). Construction of high-density linkage maps of *Populus deltoides* × *P. simonii* using restriction-site associated DNA sequencing. *PLoS ONE*, *11*, e0150692. https://doi.org/10.1371/journal.pone.0150692

Tortereau, F., Servin, B., Frantz, L., Megens, H.-J., Milan, D., Rohrer, G., … Groenen, M. (2012). A high density recombination map of the pig reveals a correlation between sex-specific recombination and GC content. *BMC Genomics*, *13*, 586. https://doi.org/10.1186/1471-2164-13-586

Trucchi, E., Frajman, B., Haverkamp, T. H. A., Schönswetter, P., & Paun, O. (2017). Genomic analyses suggest parallel ecological divergence in *Heliosperma pusillum* (Caryophyllaceae). *New Phytologist*, *216*, 267–278. https://doi.org/10.1111/nph.14722

Van Doren, B. M., Campagna, L., Helm, B., Illera, J. C., Lovette, I. J., & Liedvogel, M. (2017). Correlated patterns of genetic diversity and differentiation across an avian family. *Molecular Ecology*, *26*, 3982–3997. https://doi.org/10.1111/mec.14083

Viera, A., Santos, J. L., & Rufas, J. S. (2009). Relationship between incomplete synapsis and chiasma localization. *Chromosoma*, *118*, 377–389. https://doi.org/10.1007/s00412-009-0204-x

Vincenten, N., Kuhl, L. M., Lam, I., Oke, A., Kerr, A. R. W., Hochwagen, A., … Marston, A. L. (2015). The kinetochore prevents centromere–proximal crossover recombination during meiosis. *eLife*, *4*, e10850.

Wang, L., Bai, B., Liu, P., Huang, S. Q., Wan, Z. Y., Chua, E., … Yue, G. H. (2017). Construction of high-resolution recombination maps in Asian seabass. *BMC Genomics*, *18*, 63. https://doi.org/10.1186/s12864-016-3462-z

Wang, S., Chen, J., Zhang, W., Hu, Y., Chang, L., Fang, L., … Thang, T. (2015a). Sequence-based ultra-dense genetic and physical maps reveal structural variations of allopolyploid cotton genomes. *Genome Biology*, *16*, 108. https://doi.org/10.1186/s13059-015-0678-1

Wang, X., Yu, K., Li, H., Peng, Q., Chen, F., Zhang, W., … Zhang, J. (2015b). High-density SNP map construction and QTL identification for the apetalous character in *Brassica napus* L. *Frontiers in Plant Science*, *6*, 1164.

Wilfert, L., Gadau, J., & Schmid-Hempel, P. (2007). Variation in genomic recombination rates among animal taxa and the case of social insects. *Heredity*, *98*, 189–197. https://doi.org/10.1038/sj.hdy.6800950

Wolf, K. W. (1994). How meiotic cells deal with non-exchange chromosomes. *BioEssays*, *16*, 107–114. https://doi.org/10.1002/(ISSN)1521-1878

Wong, A. K., Ruhe, A. L., Dumont, B. L., Robertson, K. R., Guerrero, G., Shull, S. M., … Neff, M. W. (2010). A comprehensive linkage map of the dog genome. *Genetics*, *184*, 595–U436. https://doi.org/10.1534/genetics.109.106831

Wu, G. A., Prochnik, S., Jenkins, J., Salse, J., Hellsten, U., Murat, F., … Rokhsar, D. (2014). Sequencing of diverse mandarin, pummelo and orange genomes reveals complex history of admixture during citrus domestication. *Nature Biotechnology*, *32*, 656–662. https://doi.org/10.1038/nbt.2906

Xiang, Y. B., Miller, D. E., Ross, E. J., Alvarado, A. S., & Hawley, R. S. (2014). Synaptonemal complex extension from clustered telomeres mediates full-length chromosome pairing in *Schmidtea mediterranea*. *Proceedings of the National Academy of Sciences of the United States of America*, *111*, E5159–E5168. https://doi.org/10.1073/pnas.1420287111

Xu, P., Zhang, X., Wang, X., Li, J., Liu, G., Kuang, Y., … Sun, X. (2014). Genome sequence and genetic diversity of the common carp, *Cyprinus carpio*. *Nature Genetics*, *46*, 1212–1219. https://doi.org/10.1038/ng.3098

Yan, H. H., Jin, W. W., Nagaki, K., Tian, S. L., Ouyang, S., Buell, C. R., … Jiang, J. M. (2005). Transcription and histone modifications in the recombination–free region spanning a rice centromere. *Plant Cell*, *17*, 3227–3238. https://doi.org/10.1105/tpc.105.037945

Zhang, G., Liu, X., Quan, Z., Cheng, S., Xu, X., Pan, S., … Wang, J. (2012). Genome sequence of foxtail millet (*Setaria italica*) provides insights into grass evolution and biofuel potential. *Nature Biotechnology*, *30*, 549–554. https://doi.org/10.1038/nbt.2195

Zickler, D., & Kleckner, N. (2016). A few of our favorite things: Pairing, the bouquet, crossover interference and evolution of meiosis. *Seminars in Cell and Developmental Biology*, *54*, 135–148. https://doi.org/10.1016/j.semcdb.2016.02.024

## SUPPORTING INFORMATION

Additional supplemental material may be found online in the Supporting Information section at the end of the article.

**How to cite this article:** Haenel Q, Laurentino TG, Roesti M, Berner D. Meta-analysis of chromosome-scale crossover rate variation in eukaryotes and its significance to evolutionary genomics. *Mol Ecol*. 2018;27:2477–2497. https://doi.org/10.1111/mec.14699